NSWC/WOL/TR 76-7

NSWC/WOL/TR 76-7

# NSWC TECHNICAL REPORT

WHITE OAK LABORATORY

## THE EFFECT OF MOISTURE ON CARBON FIBER REINFORCED EPOXY COMPOSITES I DIFFUSION

BY
Joseph M. Augl
Alan E. Berger
NAVAL SURFACE WEAPONS CENTER
WHITE OAK LABORATORY
SILVER SPRING, MARYLAND 20910

27 SEPTEMBER 1976

- Approved for public release; distribution unlimited

NAVAL SURFACE WEAPONS CENTER
WHITE OAK, SILVER SPRING, MARYLAND 20910

UNCLASSIFIED

SECURITY CLASSIFICATION OF THIS PAGE (When Data Entered)

| REPORT DOCUMENTATION PAGE | READ INSTRUCTIONS BEFORE COMPLETING FORM |
|---|---|
| 1. REPORT NUMBER: NSWC/WOL/TR-76-7 | 2. GOVT ACCESSION NO. / 3. RECIPIENT'S CATALOG NUMBER |
| 4. TITLE (and Subtitle): The Effect of Moisture on Carbon Fiber Reinforced Epoxy Composites - I. Diffusion | 5. TYPE OF REPORT & PERIOD COVERED: Final 1 Jul 74 - 1 Jan 76 / 6. PERFORMING ORG. REPORT NUMBER |
| 7. AUTHOR(s): Joseph M. Augl, Alan E. Berger | 8. CONTRACT OR GRANT NUMBER(s) |
| 9. PERFORMING ORGANIZATION NAME AND ADDRESS: Naval Surface Weapons Center, White Oak Laboratory, White Oak, Silver Spring, Maryland 20910 | 10. PROGRAM ELEMENT, PROJECT, TASK AREA & WORK UNIT NUMBERS: 61153N; WR02204; WR0220401; WR3911 |
| 11. CONTROLLING OFFICE NAME AND ADDRESS | 12. REPORT DATE: 27 September 1976 / 13. NUMBER OF PAGES: 66 |
| 14. MONITORING AGENCY NAME & ADDRESS (if different from Controlling Office): (16) WR02204 (17) WR0220401 | 15. SECURITY CLASS. (of this report): UNCLASSIFIED / 15a. DECLASSIFICATION/DOWNGRADING SCHEDULE |

16. DISTRIBUTION STATEMENT (of this Report)

Approved for Public Release; Distribution Unlimited

17. DISTRIBUTION STATEMENT (of the abstract entered in Block 20, if different from Report)

18. SUPPLEMENTARY NOTES

19. KEY WORDS (Continue on reverse side if necessary and identify by block number)

Composites
Moisture effects
Diffusion
Carbon fiber composites

20. ABSTRACT (Continue on reverse side if necessary and identify by block number)

Mathematical models are suggested for calculating the reduced moisture diffusivities in unidirectional carbon fiber reinforced composites with hexagonal and tetragonal fiber alignment, parallel and perpendicular to the fiber direction, as a function of fiber volume fraction.

341 576

DD FORM 1 JAN 73 1473 EDITION OF 1 NOV 65 IS OBSOLETE
S/N 0102-LF-014-6601

UNCLASSIFIED
SECURITY CLASSIFICATION OF THIS PAGE (When Data Entered)

The effective diffusion coefficients measured perpendicular to the fiber direction of 6 carbon fiber composites were determined as a function of temperature and relative humidity.

The knowledge of the diffusion coefficients as a function of temperature, relative humidity, fiber volume fraction and composite geometry allow the prediction of the internal moisture distribution in a composite if the environment can be specified. A few simple examples have been illustrated.

NSWC/WOL/TR 76-7 27 September 1976

The Effect of Moisture on Carbon Fiber Reinforced Epoxy Composites. I Diffusion.

The observation by earlier investigators that the flexural and shear strengths carbon fiber reinforced composites may deteriorate at ambient storage condition made it necessary to investigate these phenomena more closely in order to get a better understanding, and ultimately, to be able to predict how these materials would behave in longtime service and storage conditions.

The work described in this report is a part of this investigation. It describes the diffusion of moisture in carbon fiber composites which may serve as a basis for prediction of longtime composite changes in various environments.

This program was funded by the Naval Air Systems Command (Task No. A3200000010123) during the periods of 1 July 1974 to 1 January 1976.

J. R. DIXON
Materials Division

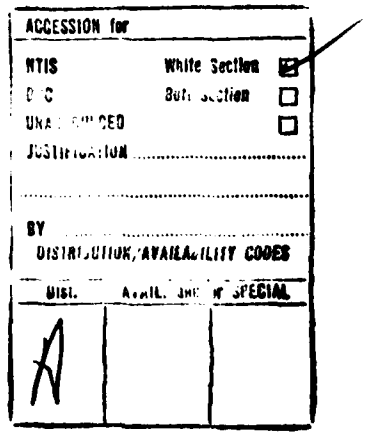

TABLE OF CONTENTS



Tables



Illustrations

ILLUSTRATIONS (Cont.)

ILLUSTRATIONS (Cont.)

## INTRODUCTION

The use of carbon fiber reinforced composites for primary and secondary structural components in aircraft construction promises not only benefits in weight savings, and with it, maneuverability and range of the aircraft, but also a considerable savings in labor cost. This savings in labor cost more than compensates for the higher cost of the raw materials.

Serious consideration is given today to the replacement of various components in aircraft with carbon fiber composites. For instance, the Lockheed Aircraft Corporation has decided to use carbon fiber-epoxy composites in the future for the vertical stabilizer of their 1011 commercial airliner. It is true that while the demands of commercial aircraft are less severe, than those of military aircraft the above use also indicates that confidence in these advanced composites has increased over the past few years. Therefore, it becomes even more necessary to learn as much as possible about these materials, such as their behavior in various environments and the change of properties with time.

This report describes part of an investigation to highlight certain aspects of environmental property changes in carbon fiber reinforced composites. There are a number of mechanisms that can lead to changes of composite properties. In this investigation emphasis was given to the effect of moisture on these composites, since the rate of moisture absorption at ambient conditions is considerably higher than the rate of any other mechanism that may lead to property changes in benign environments. Specifically, the subject of this report is the diffusion process of moisture in high performance carbon fiber reinforced composites. Diffusion coefficients were determined on several composite systems as a function of the relative humidity and temperature. These data serve as basis for estimating the moisture distribution inside the composites as functions of composite thickness, time and temperature. The concomitant composite property changes will be described in a subsequent technical report.

## BACKGROUND INFORMATION

The effect of moisture on high temperature properties of carbon fiber epoxy composites was discovered jointly by investigators of the Fiberite and Aerospace Corporation and is well

documented in a summary report by J. Hertz [1]. C. C. Browning [2] at the Air Force Materials Laboratory (AFML) compared composites with different fiber orientations and showed that the properties which are most strongly affected by moisture are the matrix controlled properties.

In earlier reports, R. Simon et al. [3] at the Naval Surface Weapons Center had investigated the effect of water on various carbon fiber composites and concluded that mechanical property changes are affected by both the nature of the carbon fiber and the type of resin used.

The longterm degradation effects on fiber reinforced composites can be caused by various mechanisms. Which mechanisms predominate depends, of course, on the type of materials that constitute the composite. In fiber reinforced composites a degradation of the resin, the fiber or the interfacial bonding will have a pronounced effect on various composite properties.

There are a number of mechanisms that can lead to composite property changes which may be differentiated as reversible and irreversible changes.

Chemical and mechanical matrix degradation such as photo-oxidation, thermal degradation (in the presence or absence of air), hydrolytic polymer chain cleavage, high energy radiaiton, stress cracking, microbial degradation, and thermal [4] and mechanical cycling may lead to irreversible property changes of fiber reinforced composites.

We define reversible property changes as those changes that can be reversed to the original properties (at least within the limitations of the sensitivity of the measurements).

A trivial case of a reversible property change is a change due to temperature, as long as the temperature change is not too high which could lead to an irreversible degradation.

Another reversible change in composite properties is observed when small molecules such as moisture or organic molecules penetrate the matrix and plasticize it. The effect of such a plasticization

---

[1] J. Hertz, Final Report NASA8-27435, June 1973 (NASA Contract).
[2] C. E. Browning, 28th Annual Conference of the Society of the Plastic Industry, Feb 1973 (Washington, D.C.); Proceedings 15A.
[3] R. A. Simon and S. P. Prosen, NOLTR 68-132, Oct 1968; M. L. Santelli and R. A. Simon, NOLTR 70-258, Feb 1971.
[4] E. L. McKagne, Jr., J. E. Halkias and J. D. Reynolds, "Moisture in Composites: "Effects of Supersonic Service on Diffusion," J. Comp. Materials, 9, 2, (1975).

is a reduction in the glass transition temperature ($T_g$) of the matrix and also a reduction in the matrix modulus over a wide temperature range. By heating and/or evacuating of such materials one can remove the moisture again and the original strength properties may be regained.

The fact that this reaction is reversible is of little practical, value, since the strength properties of a large structure cannot be easily restored. On the other hand, the composite strength is expected to deteriorate only to a certain level depending on the equilibrium conditions, which are governed by the environment, especially by the relative humidity.

The Experimental section will briefly describe the materials we have investigated and the techniques for measuring the diffusion coefficients. The following Discussion section will focus on the moisture diffusion in composite materials, while the resulting changes in mechanical properties will be described in a subsequent report.

## EXPERIMENTAL

### Materials

A. Resins

1. Narmco 5208. This resin was obtained from the Whittaker Corporation, Narmco Division. It is a one-component system (resin plus curing agent).

2. DER 332/DADS. The resin system consists of 100 parts of DER 332 (a diglycidyl ether of bisphenol A) and 36 parts of DADS (4,4' diaminodiphenyl sulfone).

3. Epon 1031/NMA. This resin consists of 100 parts of Epon 1031 [1,1,2,2-tetra(p-glycidyloxyphenyl) ethane ], 77 parts of Nadic methyl anhydride, and 1 part of BDMA (benzyldimethyl amine).

B. Fibers

1. Thornel 300. This material was obtained from Union Carbide Corporation and consists of a continuous strand of 3,000 filaments which have an epoxy sizing for better handleability. (For properties reported by the manufacturer see Table 1.)

2. HMS fibers. This material is a tow with 10,000 continuous filaments manufactured by the Hercules Corporation. The fibers had no sizing. (For properties reported by the manufacturer see Table 1.)

C. Composites

The composites were made from 8 plies of 9-inch wide prepregs, which were layed up unidirectionally and molded (in a vacuum bag) under 100 psi pressure. The details of the prepregging operation and the composite curing conditions will be described in a forthcoming technical report that will deal with the moisture and temperature effects on the mechanical properties of these composites.

Table 1: Carbon Fiber Properties

| Properties | Hercules HMS | Thornel 800 |
|---|---|---|
| Strand Modulus, psi x $10^6$ (G Pasc.) | 50 - 55 (345 - 379) | 33 - 34.5 (227 - 238) |
| Strand Break Strength, psi x $10^3$ (G Pasc.) | 340 (2.34) | 361 (2.49) |
| Density, g/cc (lot average) | 1.85 - 1.90 | 1.74 - 1.78 |
| Filament Diameter, microns | 7.2 - 7.5 | 8 |
| Number of Filaments | 10,000 | 3,000 |

## Measurements

A. Equilibrium Concentrations. To determined the moisture equilibrium concentrations of the resins and composites fine machine shavings were obtained and dried for 48 hours at 120°C in vacuum. The dried shaving samples were stored over magnesium perchlorate desiccant before use. One gram samples were prepared in individual crucibles. The sample exposure during the weighing operation was kept below 3 minutes. The samples were then exposed to 30% and 80% RH, at 30°, 45°, 60°, and 75°C.

The equilibrium concentration was defined as the concentration when the weight increase vs. time curve leveled out, which generally occurred within a few days. The percent weight gain after two weeks was designated the equilibrium concentration.

B. Fractional Weight Increase. 5 x 5 cm square samples were machined from the composite panels and sealed around the edges with a strip of aluminum foil (adhesively bonded). These specimens were dried for 72 hours at 125°C before exposure in the humidity chambers (30% and 80% RH, at 30°, 45°, 60° and 75°C). The plate samples were removed after various time intervals and the fractional weight increase $[M_t(\%)/M_\infty(\%)]$ was plotted vs. square root of time, where $M_t$ is the percent weight increase after the time(t) and $M_\infty$ is the equilibrium value.

### Humidity Chambers

The samples were put into a sample holder and placed in a wide-mouth screw cup container (23.5 cm high, 11.5 cm diameter). Various salt solutions (2 cm high, with undissolved solute) served to keep the relative humidity constant. The exposure chambers were closed and submerged into 4 water baths held at 30°, 45°, 60°, and 75°C ($\pm$.2°C).

## DISCUSSION AND RESULTS

### A. Materials

Considerations of aerodynamic heating which predicted that parts of the aircraft may reach 350°F (177°C) during supersonic flight made it mandatory that the composite materials to be used for these aircraft be stable at this temperature. Composites with 177°C performance capability require resin matrices with a glass transition temperature, $T_g$, > 177°C, i.e., resins that have no considerable loss of modulus below this temperature. Because absorption of moisture leads to a plasticization of the matrix it was expected that resins with low moisture affinity would show a better strength retention than those with high moisture saturation values.

This work was restricted to the investigation of six composite systems made from two different carbon fibers and three resins.

The resins were: Narmco 5208, DER 332/DADS and Epon 1031/NMA. The fibers were Thornel 300 and HMS fiber.

During the original screening of resins by torsional braid analysis for their thermomechanical behavior, we found that several other resins also fulfilled the temperature requirements. Some of the properties of these resins are listed in Table 2.

Two of these resins, Fiberite 904 and X-801, are no longer commercially available. The choice of resins for this investigation was somewhat arbitrary. For purposes of scientific understanding those resins whose chemical composition was known were preferred. Nevertheless, Narmco 5208, a proprietary commercial material was also included because of its attractive properties. (Hercules 3501 appeared similarly attractive; we intend to investigate this material at a later time.)

The choice of carbon fibers was based mainly on the similarity in tensile properties and on their dissimilarity in modulus (the manufactures' data are given in Table 1).

B. Effect of Moisture on Composite Strength

The change of composite strength as a function of temperature and moisture will be the subjects of two forthcoming technical reports. It will suffice here to summarize what might be expected if a composite is exposed to humidity.

At ambient temperature the rate of degradation of composite strength due to oxidation or hydrolysis is very small compared to that of moisture absorption. Thus it should be possible to predict the ultimate strength and modulus changes which are reached when the moisture content in the composite is in equilibrium with its surrounding. This equilibrium, of course, is a function of the temperature and of the relative humidity. The degradation of composite properties is expected to be a function of the absorbed moisture:

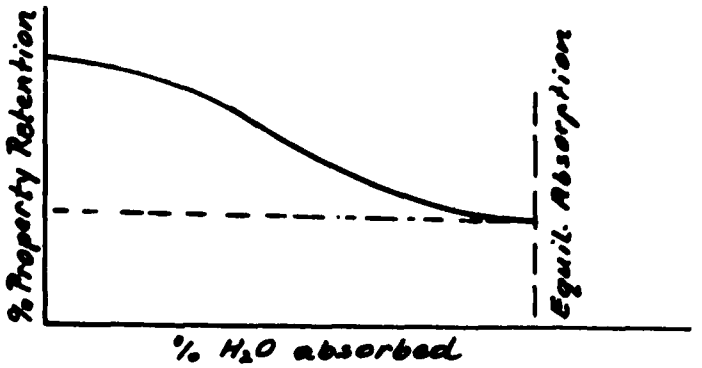

Table 2: Properties of Epoxy Resin Candidates

| Resin | Cure Cycle | Rockwell "E" Hardness | Density g/cc | Percent Moisture Pickup[1] | $T_g$[10] | $T_1$[11] | $T_2$[12] | $T_1-T_p$[13] |
|---|---|---|---|---|---|---|---|---|
| DER 332[2] + DADS[3] | 24 hr at 125°C + 4 hr at 200°C | 70 | 1.237 | 4.14 | 230 | 177 | 213 | 0 |
| Fiberite 934[4] | 3 hr at 95°C + 4 hr at 150°C | 93 | 1.294 | 4.69 | 237 | 170 | 215 | -2 |
| X-801[5] NMA[6] | 4 hr at 100°C 6 hr at 260°C | 105 | 1.251 | 3.48 | 320[15] | 265 | 283 | +88 |
| XD-7342[5] DADS[3] | 16 hr at 100°C 24 hr at 200°C | 103 | 1.230 | 5.41 | 305[15] | 200 | -- | +23 |
| NARMCO 5208[7] | 16 hr at 100°C + 3 hr at 150°C + 4 hr at 200°C | 104 | 1.247 | 6.4 | 261 | 200 | 232 | +23 |
| X-801[5] TONOX[8] | 16 hr at 23°C + 4 hr at 200°C | 100 | 1.255 | 7.31 | 235 | ?[14] | ?[14] | ?[14] |
| X-801[5] DADS[3] | 24 hr at 100°C + 4 hr at 200°C | 102 | 1.304 | 7.15 | 258 | 200 | 225 | +23 |
| Fiberite 904[4] | 3 hr at 150°C 4 hr at 200°C | 85 | 1.233 | 1.71 | 315[15] | 245 | 290 | +68 |
| 1031[9] NMA[6] | 3 hr at 125°C 5 hr at 250°C | 128 | 1.249 | 2.98 | 311[15] | 205 | 272 | +28 |
| HERCULES 3501 | 4 hr at 127°C 2 hr at 260°C | | | | 240 | 182 | 225 | +5 |

1. Determined at room temperature and 95% relative humidity on ground samples
2. Diglycidyl ether of bisphenol A
3. Diaminodiphenyl sulfone
4. Supplied by Fiberite Corp.
5. Experimental resin from Shell
6. Nadic methyl anhydride
7. Supplied by Whittaker Corp., Narmco Div.
8. A 60/40 mixture of methylenedianiline and metaphenylenediamine
9. Supplied by Shell
10. $T_g$ is the glass transition temperature defined as the temperature of maximum mechanical damping (by TBA)
11. $T_1$ is the temperature where the loss in modulus deviates from a straight line
12. $T_2$ is the point of intersection of the flat and steep branch of the modulus curve
13. $T_p$ is the maximum performance temperature to be expected under service conditions i.e., 350°F (177°C)
14. Since the modulus curve has no straight portion $T_1$ and $T_1$-$T_p$ have no defined meaning
15. $T_g$ is uncertain since the resin starts to decompose at this temperature

Thus, in order to estimate the strength degradation of composites as a result of long term exposure to the environment, specifically to humidity, at least two things must be determined:

1. The strength (or modulus) retention as a function of temperature and the amount of moisture absorbed.

2. The rate of moisture absorption (diffusion) as a function of temperature and relative humidity. Knowing the rate should allow one to predict how long it takes to reach a certain change in strength.

Of course, different strength parameters such as tensile strength, flexural strength, shear strength, compressive strength and their corresponding moduli are affected differently for the same change in moisture concentration. Also, it is assumed that a certain moisture content in the composite corresponds always to only one strength (modulus) value independent of the way the moisture was allowed to be absorbed in the sample. There is experimental evidence that the strength changes with moisture pick-up are the same whether the sample was moisture loaded by a water boil test or by water soak at ambient temperature [5]. This fact might be expected as long as the moisture concentration distribution is the same in the interior of the composite. The same overall moisture concentration might also correspond to different interior distributions, in which case there may or may not be only one strength value for a given value of percent moisture.

The time to reach a certain moisture concentration (or better, moisture distribution) is, of course, dependent on the composite geometry and the temperature and humidity profile, but can be calculated in principle if the diffusion coefficients (and their temperature and concentration dependences) are known.

Thus, one of the very important parameters to be measured for the prediction of property changes in composites is their effective diffusion coefficients of moisture along the principal axes of diffusion. Of special interest is the diffusion coefficient across the fiber direction because of the sheet geometry of most composites.

## C. Methods For Determining Diffusion Coefficients in Polymers

The two most widely applicable methods for measuring diffusion coefficients (D) are based on either steady state flow rate

[5] Personal communication with N. Judd Royal Aircraft Establishment, Farnborough, England, and Hercules, Inc.

determinations through a membrane or on the analysis of sorption data [6 to 8].

The flux (J) through a membrane is described by equations 1a and 1b.

$$J = -D_c \frac{dc}{dx} \tag{1a}$$

$$\int_0^{\ell} J dx = \int_{C_\ell}^{C_o} D_c dc \tag{1b}$$

where $D_c$ = the diffusion coefficient (which may depend on concentration), c = concentration, x = distance through the membrane.

In a steady state condition the flux is independent of x and equation (2) follows.

$$J = \frac{1}{\ell} \int_{C_\ell}^{C_o} D_c dc \tag{2}$$

The dependence of $D_c$ on concentration can be determined by measuring the flux at different concentrations on one side of the membrane while the other side is kept essentially at zero concentration.

The other method for determining D is based on absorption or desorption measurement of the diffusant in plate, sphere or rod samples.

The solution of Fick's second equation of diffusion (3)

$$\frac{\partial c}{\partial t} = D \left[ \frac{\partial^2 c}{\partial x^2} + \frac{\partial^2 c}{\partial y^2} + \frac{\partial^2 c}{\partial z^2} \right] \tag{3}$$

[6] J. Crank, "The Mathematics of Diffusion", Oxford Univ. Press. 1956.
[7] J. Crank and G. S. Parks, "Diffusion in Polymers" Acad. Press (1968).
[8] G. J. Van Amerongen, "Diffusion in Elastomers," Rubber Chem. and Techn. 37, 1065, (1964).

for a two-dimensional plate with infinite extension and exposure to constant concentration $C_1$ and $C_2$ of the diffusant on either sides and with constant initial internal concentration $C_o$ can be expressed by the series solution (4) [6].

$$\frac{M_t}{M_\infty} = 1 - \frac{8}{\Pi^2} \sum_{m=o}^{\infty} \frac{1}{(2m+1)^2} \exp\left[-D(2m+1)^2\Pi^2 t/\ell^2\right] \qquad (4)$$

where

$M_t$ = Weight increase after time t, $M_\infty$ = Weight increase at saturation level, $\ell$ = thickness of plate.

For Fickean behavior of diffusion the plot of $M_t/M_\infty$ vs. $t^{1/2}$ is practically a straight line up to a value of 0.6 of $M_t/M_\infty$. Thus, the initial absorption or desorption curves of uniformly loaded plate specimens can be used to determine D by either expression (5) (p. 241 of [6]) or (6).

$$D = 0.049/(t/\ell^2)_{1/2} \qquad (5)$$

where the subscript $1/2$ indicates that t is taken as the time for $M_t/M_\infty$ to reach the value 0.5.

$$\frac{M_t}{M_\infty} = \frac{4}{\Pi^{1/2}} \left(\frac{Dt}{\ell^2}\right)^{1/2} \qquad (6)$$

If the initial gradient, $G = d(M_t/M_\infty)/d(t/\ell^2)^{1/2}$, is observed in a sorption experiment in which D is concentration-dependent, then the average diffusion coefficient, $\bar{D}$, deduced from (6) is

$$\bar{D} = \frac{\Pi}{16} G^2 \qquad (7)$$

We have used this expression to calculate the diffusion coefficients from the sorption measurements.

D. Diffusion of Moisture in Fiber Reinforced Composites

Since composites are anisotropic media Fick's second law of diffusion takes a more complicated form (8) than for isotropic media (3). The diffusion coefficient $D_{nm}$ has a tensor form.

$$\frac{\partial c}{\partial t} = D_{11} \frac{\partial^2 c}{\partial x^2} + D_{22} \frac{\partial^2 c}{\partial y^2} + D_{33} \frac{\partial^2 c}{\partial z^2} + (D_{23} + D_{32}) \frac{\partial^2 c}{\partial y \, \partial z} +$$

$$(D_{31} + D_{13}) \frac{\partial^2 c}{\partial z \, \partial x} + (D_{12} + D_{21}) \frac{\partial^2 c}{\partial x \, \partial y} \qquad (8)$$

where x, y and z are Cartesian coordinates.

Equation (8) can be transformed into one with three principal axes of diffusion, with principal diffusion coefficients $D_1$, $D_2$, and $D_3$ and (8) can be expressed by (9)

$$\frac{\partial c}{\partial t} = D_1 \frac{\partial^2 c}{\partial \xi^2} + D_2 \frac{\partial^2 c}{\partial \eta^2} + D_3 \frac{\partial^2 c}{\partial \zeta^2} \qquad (9)$$

where $\xi$, $\eta$, $\zeta$, are the principal axes. Various symmetry considerations such as found in crystallographic systems may lead to still simpler expressions.

In a system with more than one solid component, such as a filled plastic or a fiber reinforced composite, the overall diffusion is obviously dependent on the diffusion in both substances, on the equilibrium distribution of diffusant in substance A and B as expressed by the distribution coefficient $k = C_A/C_B$, and on the spatial arrangement of A and B in the solid phase.

## E. Effective Diffusion Coefficient in Unidirectional Carbon Fiber Composites

From the symmetry of unidirectional carbon fiber composites two of the three principal diffusion coefficients are shown to be equal (see Figure 1a). The question to be answered is, how do the rates of diffusion change with respect to the unfilled matrix as we change the fiber content and the fiber direction.

If the diffusion of moisture in the carbon fiber is negligible compared with that in the resin, the problem is simplified. A further assumption is that there are no voids in the resin or between resin and fiber and that there is no significant mass transport along the resin/fiber interface.

In compacting fibers in a resin under pressure there is a higher probability for the fibers to assume a hexagonal packing (Figure 1b) than a tetragonal arrangement (Figure 1c), although in a real composite a mixed geometry due to many latice defects probably exists.

The reduced diffusivity parallel to the fiber direction in a carbon fiber epoxy composite with hexagonal fiber arrangement is the ratio of the effective diffusion coefficient to the diffusivity of the unobstructed resin.

$$\frac{D_{e\,\text{‖}\,h}}{D_r} = 1 - V_f \tag{14}$$

For a tetragonal fiber arrangement one can arrive at similar relations (from Figure 1c) as indicated below

$$V_f = \frac{\pi r^2}{(2r + d)^2} \tag{15}$$

$$\frac{r}{2r + d} = \sqrt{\frac{V_f}{\pi}} \tag{16}$$

$$\left(\frac{d}{r}\right)_t = \frac{1.7724}{V_f} - 2 \tag{17}$$

$$\frac{D_{et\,\text{‖}}}{D_r} = 1 - V_f \tag{18}$$

The fiber volume fraction for the highest packing density (d=0) for composites with hexagonal fiber arrangement is $\pi\sqrt{3}/6$ and with tetragonal arrangement it is $\pi/4$.

The ratios of d/r for the hexagonal and tetragonal fiber arrangements as a function of percent fiber volume is shown in Figure 2.

Effective diffusion coefficients for diffusion of water vapor across the fiber direction in a composite material with a hexagonal or tetragonal arrangement of fibers may be determined numerically by solving a Poisson equation (with appropriate boundary conditions) on a unit cell of the material (a detailed demonstration that it

To simplify the discussion, we consider a two-dimensional plate through which moisture diffuses under steady state conditions. If there are no fibers in the matrix the amount of material diffusing through the plate is given by Fick's first law

$$J_r = -D_r \frac{\Delta c}{\ell} \tag{10}$$

where $J_r$ = flux in $g/cm^2$ sec through the surface vertical to the flow direction, $D_r$ = average diffusion coefficient of the resin, $\Delta C$ = difference in concentration of the diffusant on both matrix surfaces, $\ell$ = thickness of the sheet.

If fibers are introduced into the matrix parallel to the flow direction, the effective cross section for the diffusion is reduced proportionally to the cross sectional area of the introduced fibers, i.e., proportionally to the fiber volume fraction, $V_f$.

The cross sectional area of the fibers with respect to a unit cell of a hexagonal fiber arrangement is $\phi_{fh} = r^2\Pi/2$ (where $r$ = radius of fiber). The total cross sectional area of the unit cell is $\phi_{tot\ h} = (2r + d)^2(\sin 60)/2$. The fiber volume fraction is therefore

$$V_f = \frac{\Pi}{\sin 60} \times \frac{r^2}{(2r + d)^2} = 3.6276 \frac{r^2}{(2r + d)^2} \tag{11}$$

The volume fraction of the resin matrix is $V_r = 1 - V_f$. The subscripts h or t refer to hexagonal or tetragonal fiber arrangements, and the subscript f and r refer to fiber and resin respectively.

From (11) follows

$$\frac{r}{2r + d} = .52503\sqrt{V_f} \tag{12}$$

and

$$\left(\frac{d}{r}\right)_h = \frac{1.9046}{\sqrt{V_f}} - 2 \tag{13}$$

where d = shortest distance from fiber to fiber surface.

is sufficient to solve only within a unit cell is given in Appendix A). Unit cells for computing the effective diffusion coefficient of water vapor perpendicular to the fibers in a hexagonal and in a tetragonal array are shown in Figure 1.

To determine the effective diffusion coefficient $d_e$ (in the y direction) with either a hexagonal or tetragonal arrangement of the fibers, we consider the following. Allow no diffusion across the vertical sides of the unit cell. Let the bottom and top faces of the unit cell be exposed to uniform concentrations of water vapor so that the water vapor concentration in the matrix along the bottom face is a constant $C_2$ and so that the water vapor concentration in the matrix along the top face is a constant $C_1$. A steady state concentration water vapor, $C(x,y)$, will then become established in the unit cell. The effective diffusion coefficient $d_e$ is given by

$$d_e = -q \cdot \bar{y}/(C_1 - C_2)(r + d/2) \tag{19}$$

where $\bar{y}$ is the height of the unit cell, and q is the flux through any y=constant surface in the unit cell (q being independent of y in the steady state). Letting $\bar{d}(x,y) \equiv D_f$ (the diffusion coefficient of the fiber) if (x,y) is a point lying in the fiber, and letting $\bar{d}(x,y) \equiv D_r$ (the diffusion coefficient of the resin) if (x,y) is a point in the resin, one has that q is given by

$$q = \int_0^{r + d/2} - \bar{d}(x,y)\, c_y(x,y)dx \quad \text{for any } y\varepsilon\, [o,\bar{y}]. \tag{20}$$

The specific differential equation and boundary conditions satisfied by c(x,y) will now be given. There is a constant k (the distribution coefficient, which depends on the particular materials in the resin and in the fiber) so that at any point p lying on an interface separating the resin and fiber regions, one has

$$c_f(p)/c_r(p) = k,$$

where $C_f(p)$ ($C_r(p)$) denotes the limit at p of the concentration as one approaches from within the fiber (resin). Let the function u(x,y) be given by

$$u(x,y) = \begin{cases} c(x,y), \text{ for points } (x,y) \text{ in the resin} \\ c(x,y)/k \text{ for points } (x,y) \text{ in the fiber} \end{cases} \tag{21}$$

so then u(x,y) will be continuous across any interface between matrix and fiber. If p is a point on an interface between resin and fiber, let n denote a unit normal to the interface curve at p. Then the condition of continuity of flux at p is

$$-D_f \cdot k \cdot u_n^f(p) = -D_r\, u_n^r(p) \tag{22a}$$

where $u_n^f(p)$ ($u_n^r(p)$) denotes the normal derivative of u at p calculated from within the fiber (resin). In the case $D_f = 0$ the left side of (22a) is defined to be 0. The differential equation and other boundary conditions satisfied in the unit cell by u are;

$$0 = D_r \Delta u \equiv D_r\ (u_{xx} + u_{yy}) \text{ in the resin,} \tag{22b}$$

$$0 = D_f \cdot k\Delta u \text{ in the fiber} \tag{22c}$$

with the understanding that when $D_f = 0$ conditions on u holding in the fiber region are to be omitted,

$$u(x,o) = C_2 \text{ and } u(x,\bar{y}) = C_1 \quad \text{for } 0<x<r+d/2, \tag{22d}$$

$$u_x(o,y) = 0 \text{ and } u_x(r+d/2,y) = 0 \quad \text{for } 0\ y\ \bar{y} \tag{22e}$$

Note that (20) in terms of u is

$$q = \int_o^{r+d/2} -d(x,y)\, u_y(x,y)dx \quad \text{for any } y\varepsilon\ [o,\bar{y}], \tag{23}$$

where $d(x,y) = D_r$ in the resin and $d(x,y) = k \cdot D_f$ in the fiber.

Numerical approximation of (19), (22), and (23) was done as follows (a completely detailed discussion is given in Appendix 1). Rather than solve the interface problem (22) directly, which would involve dealing directly with the geometry of the curved interface between matrix and fiber, a variable diffusion coefficient problem (24-26) approximating (22) was solved on the rectangular unit cell;

$$u(x,o) = C_2 \text{ and } u(x,\bar{y}) = C_1 \quad \text{for } 0<x<r+d/2 \tag{24}$$

$$u_x(o,y) = 0 \text{ and } u_x(r+d/2,y) = 0 \text{ for } 0<y<\bar{y} \tag{25}$$

$$\nabla \cdot \tilde{d}\,(x,y)\nabla u = 0 \quad \text{on } 0<x<r+d/2,\ 0<y<\bar{y} \tag{26}$$

where away from the interface, $\tilde{d} = D_r$ in the resin and $\tilde{d} = k \cdot D_f$ in the fiber, while in a narrow zone near the interface d changes continuously from $D_r$ to $k \cdot D_f$. In the situation $D_f = 0$, $\tilde{d}$ was defined to be $k/1000$ in the fiber, and varied from $D_r$ to $k/1000$ near the interface.

The Equations (24-26) were solved using the D'Yakonov ADI (alternating direction implicit) finite difference method on a grid with uniform mesh spacings $\Delta x$ and $\Delta y$ in the x and y directions, respectively. The flux q given by (23) (with d(x,y)) replaced by d(x,y)) was evaluated by differencing u to obtain $u_y$ and by using the trapezoidal quadrature rule to evaluate the integral.

## F. Thermal and Electrical Analogs to Diffusion Processes

A thermal analogue to the diffusion of moisture through a medium with cylindrical obstacles perpendicular to the flow direction has been treated by G. S. Springer and S. W. Tsai [9]. These authors have calculated the thermal conductivity of a system with tetragonal arrangement of cylindrical rods embedded in a matrix with different thermal conductivity. They obtained the following equation

$$\frac{k_{22}}{k_m} = \left(1 - 2\sqrt{\frac{V_f}{\Pi}}\right) + \frac{1}{B}\left[\Pi - \frac{4}{\sqrt{1 - B^2 V_f/\Pi}} \tan^{-1}\left(\frac{\sqrt{1 - (B^2 V_f/\Pi)}}{1 + \sqrt{B^2 V_f/\Pi}}\right)\right]$$

$$B = 2\left(\frac{k_m}{k_f} - 1\right) \tag{27}$$

$k_{22}$ = thermal conductivity perpendicular to the axes of the cylinders, $k_m$ = thermal conductivity of the matrix, $V_f$ = volume fraction of the cylindrical rods.

If $k_f$ becomes zero (or for the analog in diffusion, the diffusion coefficient of the fiber becomes zero), the second term goes to zero.

At equilibrium the difference in concentration of diffusant in phase (f) and phase (r) can be expressed by the ratio

[9] G. S. Springer and S. W. Tsai, "Thermal Conductivity of Unidirectional Materials" J. Comp. Mat. 1, 166 (1967).

$k = c_f/c_r$ (the distribution coefficient between resin and fiber). If Henry's law applied, the analog $kD_f/D_r$ can be substituted for $k_f/k_r$ so that the Springer-Tsai equation becomes

$$\frac{D_{et}}{D_r} = \left(1 - 2\sqrt{\frac{V_f}{\pi}}\right) + \frac{1}{B}\left[\pi - \frac{4}{1 - \sqrt{B^2 V_f/\pi}} \tan^{-1}\left(\frac{\sqrt{1 - B^2 V_{f/\pi}}}{1 + \sqrt{B^2 V_{f/\pi}}}\right)\right]$$

$$B = 2\left(\frac{D_r}{kD_f} - 1\right) \tag{28}$$

Another analog has been calculated for an electrical conductivity problem by Lord Rayleigh [10] and Runge [11]. Again the system was composed of tetragonally arranged cylinders in a matrix with different conductivity. An equation was derived which gave the overall conductivity in terms of the conductivities of the cylinder and matrix materials

$$\frac{K}{K_m} = 1 - \frac{2V_f}{\dfrac{1 + \dfrac{K_f}{K_m}}{1 - \dfrac{K_f}{K_m}} + V_f - \dfrac{1 - \dfrac{K_f}{K_m}}{1 + \dfrac{K_f}{K_m}} V_f^4 \times 0.3058 - \ldots} \tag{29}$$

which reduces to equation (30) when the conductivity of the cylinders become zero

$$\frac{K}{K_m} = 1 - \frac{2V_f}{1 + V_f - .3058\, V_f^4 \ldots} \tag{30}$$

The conductivity in the Rayleigh equation does not become zero as it should for the highest packing density of tetragonal cylinder arrangement (see Figure 3). No explanation was given by the author.

There is a considerable difference at the lower fiber volume fractions between the Rayleigh curve and that of Springer-Tsai for zero thermal conductivity of the cylinders.

[10] Lord Rayleigh, Philosoph. May. 34, 481 (1892).
[11] I. Runge, Z. Tech. Phys. 6, 61 (1925).

The curve we obtained from the finite difference approach was in excellent agreement to that of Rayleigh (for the tetragonal fiber arrangement) up to about .70 fiber fraction. Above this density the Rayleigh equation fails. The reason why the Springer-Tsai model gives lower values of reduced diffusivities over the whole range is, that it is based on a simple thermal model where the composite elements are connected in series [9]. This means that a single fiber running through the matrix (vertical to the flow direction) has the same effect as a whole sheet of graphite with the same thickness as the fiber being placed in the flow direction.

That there is a difference can be shown by the same finite difference method if the following boundary value problems are solved:

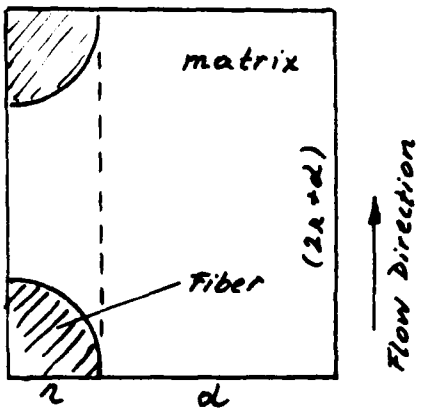


a) for the unobstructed region dx(2r+d)

b) for the region within (r+d) x (2r+d)

If this simple thermal model would be applied for the hexagonal fiber arrangement it would fail already at $\pi/8\sqrt{3}$ fiber volume fraction because this model does not take into account that the diffusant can flow around the fibers. The difference of various models is given in Table 3 and Figure 3.

## G. Diffusion Coefficient in an Arbitrary Angle to the Fiber Direction of a Unidirectional Carbon Fiber Composite

The principal axes of diffusion are parallel and perpendicular to the fiber direction. $D_e$, therefore, constitutes a rotational ellipsoid with two principal diffusion coefficients being equal. For the general case one can state that the diffusion coefficient, D, at right angles to surfaces whose normals have the direction cosines $\ell$, m, n relative to the principal axes of diffusion is given by

$$D = \ell^2 D_x + m^2 D_y + n^2 D_z \qquad (31)$$

Table 3: Reduced Diffusivities as a Function of Fiber Volume Fraction

| $V_f$ | $D_{e\parallel}/D_r$ | Finite Difference Method | | Rayleigh | Springer-Tsai | Finite Diff. Meth. | Finite Diff. Meth. |
|---|---|---|---|---|---|---|---|
| | | $D_{eh\perp}/D_r$ | $Det_\perp/D_r$ | $D_{et_\perp}/D_r$ | $D_{et_\perp}/D_r$ | $D_{et\parallel}/Det_\perp$ | $D_{eh\parallel}/D_{eh\perp}$ |
| 0 | 1 | 1 | 1 | 1 | 1 | 1 | 1 |
| .05 | .95 | - | .9053 | .906 | .7477 | 1.050 | 1.050 |
| .1 | .9 | .8189 | .8189 | .822 | .6432 | 1.099 | 1.099 |
| .2 | .8 | .6659 | .6671 | .673 | .4954 | 1.199 | 1.201 |
| .3 | .7 | .5381 | .5376 | .546 | .3819 | 1.302 | 1.301 |
| .4 | .6 | .4289 | .4260 | .435 | .2863 | 1.408 | 1.399 |
| .5 | .5 | .3351 | .3266 | .336 | .2021 | 1.531 | 1.492 |
| .6 | .4 | .2496 | .2326 | .243 | .1259 | 1.720 | 1.603 |
| .65 | .35 | .2119 | .1846 | .198 | - | 1.896 | 1.652 |
| .7 | .3 | .1710 | .1375 | .153 | .0559 | 2.182 | 1.754 |
| .75 | .25 | .1377 | .0944 | .107 | .0228 | 2.648 | 1.816 |
| .8 | .2 | .1021 | - | .059 | - | ∞ | 1.959 |
| .85 | .15 | .0663 | - | .009 | - | | 2.262 |
| .907 | .093 | 0 | - | - | - | | ∞ |

and the corresponding fluxes are

$$J_x = -D_x \frac{\partial c}{\partial x}, \quad J_y = -D_y \frac{\partial c}{\partial y}, \quad J_z = -D_z \frac{\partial c}{\partial z}$$

Thus, knowledge of $D_{e\parallel}$ and $D_{e\perp}$ is all that is required to describe diffusion in a unidirectional carbon fiber composite.

For instance, the reduced diffusivity in a unidirectional carbon fiber composite, which is rotationally symmetric in the fiber direction, can be expressed as follows.

$$\frac{D_{e\alpha}}{D_r} = D_{e\parallel} \cos^2\alpha + D_{e\perp} \sin^2\alpha \qquad (32)$$

## H. Effective Diffusion Coefficients in Cross-Plied Laminar Composites

If a composite is made of several layers of the same prepreg but with the layers laid up such that the fiber directions are different for each layer, there is basically no difference in the effective diffusion coefficient perpendicular to the fiber direction if the average fiber volume fraction is known. The reason is that a laminar ply consists usually of many layers of fibers in the same direction. The effective diffusion coefficients in various directions in the plane of the sheet is a superposition of all the single plies and their respective fiber directions. Each ply can be treated as a unidirectional composite for which $D_{e\parallel}$ and $D_e$ are known as a function of their fiber volume fraction. Of course, the angular dependence of the diffusion rates in each ply is not independent of the other plies since there is an additional requirement. In order to maintain equilibrium, the concentrations at the bounaries between plies (m and n) must be continuous. For instance, if the flow is parallel to ply m (=0°), then the flow in ply n ($\neq$ 0°) is increased because there is an outflow from m into n which has a slower rate of diffusion in this particular direction. Thus, for the same reason, the effective diffusion rate in ply m (in the 0° direction) is retarded as compared to the original rate of diffusion parallel to the fibers without neighboring plies (with different fiber directions).

## I. Measurements of the Diffusion Coefficients ($D_{e\perp}$) of Carbon Fiber Reinforced Composites

The effective diffusion coefficients ($D_{e\perp}$) of 6 carbon fiber composite systems (made of 3 resins: Narmco 5208, DER 332/DADS and Epon 1031/NMA were determined as a function of temperature and relative humidity.

a. Equilibrium Concentration of the Composites as a function of temperature and relative humidity.

Calculations show that it would take more than 100 years for the composite plate of 1 cm thickness to reach equilibrium at room temperature; therefore, the equilibrium concentration was measured on thin composite shavings. The results thus obtained compared well with calculated values from resin equilibrium measurements, also obtained from shavings or films. The calculations were made with the assumption that only the resin absorbs moisture. The constant humidity exposures of 30% and 80%RH were carried out by adjusting the humidity with various saturated salt solutions (Table 4) for different temperatures. The results are shown in Table 5. Figure 4 shows the equilibrium concentration profile of Narmco 5208 as a function of temperature and relative humidity.

The equilibrium concentration in the samples increase with increasing RH as is expected from Henry's law, which states that the saturation point is proportional to the vapor pressure. However, in some cases the equilibrium concentration seems to decrease slightly with increasing temperature at constant relative humidity in spite of the fact that at constant RH the absolute concentration of moisture in the surrounding air increases with increasing temperature (see Figure 5). The reason for the lower equilibrium concentration at higher temperature may be due to the fact that the surface adsorption is lower at higher temperature. Thus, the equilibrium concentration of the interior seems to be governed by the surface adsorption. Water submersion may show different results.

b. Fractional Weight Absorption of Carbon Fiber Composites.

5 x 5 $cm^2$ composite plate samples, sealed around the edges with aluminum foil to prevent diffusion parallel to the fiber direction, were exposed at various constant temperatures and constant RH values. The fractional weight increases, $M_t/M_\infty$, (where $M_t$ is the percent weight increase after the exposure time t and $M_\infty$ is the percent equilibrium concentration as determined under [a]), were plotted vs. $t^{\frac{1}{2}}$ for the composite samples Epon 1031/HMS, at 30% and 80% RH at 30°, 45°, 60° and 75°C (See Figures 6 and 7).

c. Effective Diffusion Coefficients ($D_{e\perp}$) of Carbon Fiber Composites as a Function of RH and Temperature.

From the slope of the sorption curves the diffusion coefficients, $D_{e\perp}$ were calculated according to equation 7. The results are given in Table 6 and as three-dimensional projections in Figures 8 through 13.

Since the composites, made from the T300 and HMS fibers, only differ about 4 percent in fiber volume concentration, the difference in diffusion coefficients between the two sets of composites is

Table 4: Relative Humidities Above Saturated Salt Solutions At Various Temperatures[a]

| Temp. (°C) | Approx. RH | < ∿33 | < ∿55 | < ∿80 |
|---|---|---|---|---|
| 30 | | $MgCl_2$ (33) | $Na_2Cr_2O_7 \cdot 2H_2O$ (57) | $NH_4Cl$ (81) |
| 45 | | $MgCl_2$ (32) | $Na_2Cr_2O_7 \cdot 2H_2O$ (54) | $NH_4Cl$ (79) |
| 60 | | $MgCl_2$ (30) | $Na_2Cr_2O_7 \cdot 2H_2O$ (55) | KCl (80) |
| 75 | | $MgCl_2$ (29) | $Na_2CrO_4$ (56) | KCl (80) |

(a) The numbers in parentheses are the RH values reported in the literature for the respective temperatures.

Table 5

Equilibrium Concentration of Moisture in Epoxy Resins at Various Temperatures (at 30 and 80% RH)

| Resin | Exposure to (% RH) | Exposure at (°C) | Equilibrium Concentration (%) |
|---|---|---|---|
| 5208 | 80 | 30 | 4.64 |
| 5208 | 80 | 45 | 4.57 |
| 5208 | 80 | 60 | 4.50 |
| 5208 | 80 | 75 | 4.50 |
| 332 | 80 | 30 | 2.84 |
| 332 | 80 | 45 | 2.61 |
| 332 | 80 | 60 | 2.48 |
| 332 | 80 | 75 | 2.07 |
| 1031 | 80 | 30 | 1.67 |
| 1031 | 80 | 45 | 1.44 |
| 1031 | 80 | 60 | 1.23 |
| 1031 | 80 | 75 | 0.90 |
| 5208 | 30 | 30 | 1.93 |
| 5208 | 30 | 45 | 1.83 |
| 5208 | 30 | 60 | 1.80 |
| 5208 | 30 | 75 | 1.75 |
| 332 | 30 | 30 | 1.31 |
| 332 | 30 | 45 | 1.27 |
| 332 | 30 | 60 | 1.04 |
| 332 | 30 | 75 | 0.82 |
| 1031 | 30 | 30 | 0.60 |
| 1031 | 30 | 45 | 0.58 |
| 1031 | 30 | 60 | 0.52 |
| 1031 | 30 | 75 | 0.44 |
| 5208 | 100 | 30 | 5.93 |
| 5208 | 100 | 75 | 6.10 |
| 5208 | 100 | 100 | 5.98 |

The equilibrium concentrations have been determined on resin shavings, or resin films.

Table 6

Diffusion Coefficients of Various Carbon Fiber Epoxy Composites as a Function of Temperature and Relative Humidity

| Panel Number | Fiber | Resin | Exposure to % RH | Exposure Temp. (°C) | Diffusion Coeff. $cm^2/sec$ | Specimen Thickness (cm) | Fiber Volume Fraction |
|---|---|---|---|---|---|---|---|
| 6 | T300 | 5208 | 33 | 30 | 1.26 X E-11 | .213 | .703 |
| 6 | T300 | 5208 | 33 | 45 | 2.85 X E-10 | .208 | .703 |
| 6 | T300 | 5208 | 33 | 60 | 5.40 X E-10 | .203 | .703 |
| 6 | T300 | 5208 | 33 | 75 | 1.08 X E-9 | .203 | .703 |
| 18 | T300 | 332 | 33 | 30 | 1.83 X E-10 | .205 | .713 |
| 18 | T300 | 332 | 33 | 45 | 3.36 X E-10 | .216 | .713 |
| 18 | T300 | 332 | 33 | 60 | 4.81 X E-10 | .198 | .713 |
| 18 | T300 | 332 | 33 | 75 | 2.33 X E-9 | .210 | .713 |
| 28 | T300 | 1031 | 33 | 30 | 1.14 X E-9 | .213 | .692 |
| 28 | T300 | 1031 | 33 | 45 | 2.78 X E-9 | .213 | .692 |
| 28 | T300 | 1031 | 33 | 60 | 4.27 X E-9 | .213 | .692 |
| 28 | T300 | 1031 | 33 | 75 | 1.10 X E-8 | .213 | .692 |
| 24 | HMS | 5208 | 33 | 30 | 1.67 X E-10 | .226 | .687 |
| 24 | HMS | 5208 | 33 | 45 | 3.06 X E-10 | .231 | .687 |
| 24 | HMS | 5208 | 33 | 60 | 5.39 X E-10 | .227 | .687 |
| 24 | HMS | 5208 | 33 | 75 | 9.70 X E-10 | .231 | .687 |
| 21 | HMS | 332 | 33 | 30 | 2.44 X E-10 | .229 | .689 |
| 21 | HMS | 332 | 33 | 45 | 5.09 X E-10 | .231 | .689 |
| 21 | HMS | 332 | 33 | 60 | 1.07 X E-9 | .236 | .689 |
| 21 | HMS | 332 | 33 | 75 | 3.75 X E-9 | .231 | .689 |
| 26 | HMS | 1031 | 33 | 30 | 1.40 X E-9 | .241 | .671 |
| 26 | HMS | 1031 | 33 | 45 | 2.80 X E-9 | .239 | .671 |
| 26 | HMS | 1031 | 33 | 60 | 5.00 X E-9 | .234 | .671 |
| 26 | HMS | 1031 | 33 | 75 | 1.01 X E-8 | .231 | .671 |
| 6 | T300 | 5208 | 80 | 30 | 1.21 X E-10 | .213 | .703 |
| 6 | T300 | 5208 | 80 | 45 | 3.64 X E-10 | .208 | .703 |
| 6 | T300 | 5208 | 80 | 60 | 8.05 X E-10 | .203 | .703 |
| 6 | T300 | 5208 | 80 | 75 | 1.11 X E-9 | .203 | .703 |
| 18 | T300 | 332 | 80 | 30 | 2.01 X E-10 | .205 | .713 |

Table 6 (Cont.)

| Panel Number | Fiber | Resin | Exposure to % RH | Exposure Temp. (°C) | Diffusion Coeff. $cm^2/sec$ | Specimen Thickness (cm) | Fiber Volume Fraction |
|---|---|---|---|---|---|---|---|
| 18 | T300 | 332 | 80 | 45 | 5.79 X E-10 | .216 | .713 |
| 18 | T300 | 332 | 80 | 60 | 1.00 X E-9 | .198 | .713 |
| 18 | T300 | 332 | 80 | 75 | 2.37 X E-9 | .210 | .713 |
| 28 | T300 | 1031 | 80 | 30 | 1.20 X E-9 | .213 | .692 |
| 28 | T300 | 1031 | 80 | 45 | 3.13 X E-9 | .213 | .692 |
| 28 | T300 | 1031 | 80 | 60 | 8.34 X E-9 | .213 | .692 |
| 28 | T300 | 1031 | 80 | 75 | 1.32 X E-8 | .213 | .692 |
| 24 | HMS | 5208 | 80 | 30 | 1.81 X E-10 | .226 | .678 |
| 24 | HMS | 5208 | 80 | 45 | 4.34 X E-10 | .231 | .678 |
| 24 | HMS | 5208 | 80 | 60 | 1.14 X E-9 | .229 | .678 |
| 24 | HMS | 5208 | 80 | 75 | 1.49 X E-9 | .231 | .678 |
| 21 | HMS | 332 | 80 | 30 | 2.85 X E-10 | .229 | .689 |
| 21 | HMS | 332 | 80 | 45 | 8.62 X E-10 | .231 | .689 |
| 21 | HMS | 332 | 80 | 60 | 2.16 X E-9 | .236 | .689 |
| 21 | HMS | 332 | 80 | 75 | 3.55 X E-9 | .231 | .689 |
| 26 | HMS | 1031 | 80 | 30 | 1.33 X E-9 | .241 | .671 |
| 26 | HMS | 1031 | 80 | 45 | 4.26 X E-9 | .239 | .671 |
| 26 | HMS | 1031 | 80 | 60 | 9.35 X E-9 | .234 | .671 |
| 26 | HMS | 1031 | 80 | 75 | 2.00 X E-8 | .239 | .671 |
| -- | --- | 5208 | 33 | 30 | 1.40 X E-9 | .368 | 0.00 |
| -- | --- | 5208 | 80 | 30 | 1.42 X E-9 | .368 | 0.00 |
| -- | -- | 5208 | 100 | 30 | 1.50 X E-9 | .370 | 0.00 |
| -- | -- | 5208 | 80 | 75 | 1.17 X E-8 | .368 | 0.00 |
| -- | -- | 5208 | 33 | 75 | 8.60 X E-9 | .364 | 0.00 |
| -- | -- | 5208 | 100 | 100 | 3.75 X E-8 | .373 | 0.00 |

expected to be smaller than the experimental error of the measurement. However, if the ratios of the $D_{e\perp}$'s of the HMS/T300 composites (see Table 7) are listed, then a consistently higher $D_e$ is observed for the HMS composites of the same resins and the same exposure conditions. The diffusion coefficients for Narmco 5208, DER 332/DADS and Epon 1031/MNA HMS composites are on the average about 40%, 60% and 20%, respectively, higher than the corresponding T300 composites. The T300 fiber had an epoxy sizing for better handleability while the HMS fiber had none. This treatment of the T300 fibers with an epoxy surface coating appears to lead to a better wetting of the fibers by the resin, therefore, to a reduction of interfacial void formation. Obviously, the diffusion rates through the voids would be very much larger than if the same volume were filled with resin. The measurement of void content by the resin digestion method, however, is not sensitive enough (if differences are due to voids).

Very little is known about the interface in carbon fiber composites. The questions of whether there is a significant diffusion along the interface has, to our knowledge, not been determined. This interface may play a role similar to the grain boundaries in metals and ceramics. Low temperature diffusion of He, $H_2$ or argon might give some insight as to the microporosity, particularly along the resin-fiber interface.

d. Distribution of Moisture in Composites as a Function of Thickness, Time, Relative Humidity and Temperature.

The solution of Fick's second diffusion equation for a sheet geometry is shown in Figure 14. The solution is given in dimensionless parameters: $Dt/h^2$, the coordinates are given as $C-C_o/C_1-C_o$ and $X/h$, where D = diffusion constant, t = time h = is half the thickness of sheet, $C_o$ = initial uniform concentration, $C_1$ = concentration kept constant at the surface. This graph applies, therefore, for all substances following Fickean diffusion behavior.

Figure 15 allows very quickly, without the use of a computer, the determination of the moisture distribution inside a solid material, once the diffusion coefficient of moisture has been determined.

After integrating the $Dt/h^2$ curves of Figure 15, a plot of $M_t/M_\infty$ vs. $[Dt/h^2]^{1/2}$ (again of dimensionless parameters) can be derived. This plot, shown in Figure 15, permits the determination of the internal distribution of the diffusant by simply measuring the sample's fractional weight increase, $M_t/M_\infty$, assuming D has been previously determined. The measured $M_t/M_\infty$, corresponds to a certain $[Dt/h^2]^{1/2}$ in Figure 15 from which $Dt/h^2$ is determined and interpolated on Figure 14 to give the internal distribution.

Table 7

A comparison of the effective moisture diffusion coefficients ($D_{e\perp}$) in the HMS and T300 carbon fiber composites.

| Exposure Temp. °C | RH % | Ratio of $D_{e\perp}$ (HMS)/$D_{e\perp}$ (T300) Narmco 5208 | DER 332/DADS | Epon 1031/NMA |
|---|---|---|---|---|
| 30 | 30 | 1.88 | 1.10 | 1.05 |
| 45 | 30 | 1.60 | 1.51 | 1.36 |
| 60 | 30 | 1.56 | 2.08 | 1.29 |
| 75 | 30 | .98 | 1.61 | .92 |
| 30 | 80 | 1.50 | 1.42 | 1.11 |
| 45 | 80 | 1.12 | 1.48 | 1.36 |
| 60 | 80 | 1.27 | 2.16 | 1.12 |
| 75 | 80 | 1.16 | 1.50 | 1.51 |
| Average | | 1.38 | 1.61 | 1.21 |
| Coeff. Var | | 7.70 | 7.69 | 5.72 |
| Stand. Deviation of the Mean | | .1063 | .1238 | .0693 |

Of course, a finite difference method for calculating the distributions by means of a computer can always be employed. There is, for instance, the Crank-Nicolson method described in reference [6].

For illustrative purposes a Narmco 5208/T300 composite is considered. The samples of 1 cm thickness are exposed to a) 80% RH at 25°C, b) 30% RH and 25°C, c) 80% RH and 35°C, and also, d) a plate of 0.25 cm thickness is exposed to 35°C and 80% RH.

The moisture equilibrium concentrations at 25°C are 1.26% for 80% RH and .582% for 30% RH, and at 35°C and 80% RH the equilibrium concentration is 1.25%. The diffusion coefficients (see Figure 8) at 25°C and 30% and 80% RH are $1 \times 10^{-10}$ $cm^2/sec$ and $6 \times 10^{-11}$ $cm^2/sec$ respectively and at 35°C and 80% RH the diffusion coefficient is $\sim 2.5 \times 10^{-10}$ $cm^2/sec$.

Using Figure 14 the isochronal distribution of moisture inside the composite can be obtained for various times; these distributions are shown in Figure 16. From these graphs it is apparent that the time required for 98% saturation differs widely. Saturation times depend on the square of the thickness of the composite and on the temperature, which roughly doubles the rate for every 10°C increase in temperature.

The percent weight increase with time for these 4 conditions can be easily obtained from Figure 15 by using the relation of $M_t/M_\infty$ vs. $[Dt/h^2]^{1/2}$. The results are shown in Figure 17. For varying boundary conditions with changing temperatures and humidities the problem is more complicated but can be solved with a computer. Details of how to predict the effect of real outdoor weather conditions with constantly varying boundary conditions will be the subject of a forthcoming NSWC/TR.

Two more distributions for the DER 332/DADS-HMS and Epon 1031/NMA-HMS composites are shown in Figures 18 and 19. Both moisture distributions were calculated for a 1 cm thick plate exposed at 25°C at 80% RH.

e. Temperature Coefficients of Diffusion

The temperature coefficient of moisture diffusion for the three HMS fiber composites at 30% RH was obtained from Figure 20 where the logarithms of the diffusion coefficients were plotted vs. 1/T (°K). Since the equilibrium concentration is only slightly dependent on temperature (at least below 60°C), the slopes of these straight lines might be considered as overall activation energies of diffusion of moisture across the fiber direction. The values range from about 8 to 10 kcal/mole. Although the slopes are about the same, there is a difference of an order of magnitude

between the Epon 1031 and the Narmco 5208 composites. The diffusion rate of the Epon 1031 composite is about 10 times higher than the Narmco 5208 resin, in spite of the fact that the moisture equilibrium concentration in the 1031 composite is only 1/3 of the equilibrium concentration of Narmco 5208. Therefore equilibrium moisture absorption is not necessarily an indication of the rate of diffusion. Thus one ought to be careful in judging resins simply by their equilibrium moisture absorption.

Furthermore, as will be reported in a subsequent technical report on the mechanical property changes on these composites, a low moisture equilibrium concentration does not necessarily mean that the mechanical properties changes will be proportionally small.

f. Sample Preparation.

Since the sample's final equilibrium concentration of moisture ($M_\infty$) depends on the relative humidity of the surrounding environment, the relative humidity at which the samples have been prepared makes a difference. At the surface of the sheet of resin (or composite) the saturation level is reached within a very short time. This is governed by the surface adsorption. This may be the reason why the rate of absorption at a given temperature is different for different relative humidities (see Figure 21). Thus, samples with the same percentage of moisture content may have different distributions. For instance from Figure 21 one can see that (for a sample of 0.370 cm thickness of Narmco 5208, at 30°C, a 0.4% moisture pick-up is reached in water after 4.8 days, at 80% RH after 6.6 days, and at 30% RH after 15.5 days. Obviously, since the boundary conditions are different, so is the internal moisture distribution.

It is not yet known how the mechanical properties of composites vary, if at all, when they are prepared in different RH's but having the same total moisture concentration. Such differences in preparation will have to be considered for sample testing designed to predict the property changes in various climatic environments.

The ultimate equilibrium concentration of moisture inside the composite will correspond to the longtime average humidity in the environment. The perturbation due to short-time (daily) humidity fluctuations is restricted only to a thin surface layer on the order of $x = 2(\pi \bar{D} t_o)^{\frac{1}{2}}$, where x is the depth in change of moisture concentration due to the environmental humidity fluctuation, $\bar{D}$ is the average effective diffusion coefficient and $t_o$ is the length of the cycle. For Narmco 5208/T300 composite this distance would be 0.005 cm at ambient temperature and a humidity fluctuation around 80% RH over a 24-hour cycle.

J. Comparison With Experimental Data

There are not many numerical data published in the literature that would permit the verification of the calculated data with

experiments. Hertz [1] has measured the diffusion coefficients $D_{e\parallel}$ and $De\perp$ in a carbon fiber reinforced epoxy composite ($V_f$ = 58.8%, and 2.3% voids). The measured data were $D_{e\parallel}$ = 6.34 x $10^{-8}$ $cm^2$/sec and $D_{e\perp}$ = 1.56 x $10^{-8}$ $cm^2$/sec. Unfortunately he did not give the diffusion coefficient of the neat resin. The ratio of $D_{e\parallel}$ /$D_{e\perp}$ should be between 1.6 - 1.7 (see Table 3). The experimental ratio is 4.06, indicating $D_{e\parallel}$ is larger than should be probably because of elongated voids in the fiber direction (perhaps debonding along the fibers).

Also, the measured values of $D_{e\parallel}$ and $D_{e\perp}$ are surprisingly high. From $D_{e\perp}$ = 1.56 x $10^{-8}$ $cm^2$/sec, according to Table 3 the resin should have a diffusion coefficient of about 6.5 x $10^{-8}$ $cm^2$/sec, which is rather high for epoxy resins. Thus, even low void contents seem to have a pronounced effect on the diffusion coefficient. On the other hand the diffusion coefficients we measured on the Narmco 5208 composites (see Table 6) are all lower than the values calculated from the finite difference method. The HMS fiber composites are 17-20% lower and the T300 composites between 36-53% lower than the values calculated for a tetragonal fiber arrangement. One reason could be that the resin samples were cast from a different resin batch than the resin used for the composite preparation. We have previously observed on a different epoxy resin that within the same resin batch, a difference in thermal history (for instance different gelation temperatures but same cure and post cure) give a difference of 22% in resin diffusion coefficients. Another reason could be that the composite equilibrium values was determined on powder samples. Since these fine powders can equilibriate very rapidly there is the possibility of a weighing error due to the time required for removing the samples from the exposure chambers and weighing them.

## Conclusions and Recommendations

A finite difference method was used to estimate the reduced diffusivities in unidirectional carbon fiber composites with hexagonal and tetragonal fiber arrangement. For the tetragonal arrangement of cylindrical rods these derivations were compared with two models, derived by other investigators for the analogous electrical and thermal conductivities. While the Rayleigh model gives almost identical results with ours at fiber concentrations below 60 percent, the Springer-Tsai model deviates considerably over the whole range of fiber volume fractions.

The effective diffusion coefficients of 6 carbon fiber/epoxy composites were determined (perpendicular to the fiber direction) as a function of temperature and relative humidity. There is a reasonable agreement with the calculated reduced diffusivity for the .7 fiber volume fraction of these composites.

The effective diffusion constants for the composites follow the order $D_{(1031)} > D_{(332)} > D_{(5208)}$ while the saturation values follow the inverse order $C_{\infty(5208)} > C_{\infty(332)} > C_{\infty(1031)}$. This reversal of order indicates that measurement of moisture pickup alone is not sufficient for determining the effect of moisture on resins or composites.

Diffusion processes should be further investigated since diffusion measurements seem to be quite sensitive to composite changes (that can generate micro cracks) and which might not be readily detected by mechanical testing. Furthermore, diffusion measurements should be combined with mechanical and thermal cycling experiments.

In addition to moisture diffusivities, we expect that low temperature He, Ar, or $H_2$ diffusivities may give gome additional information about the resin-fiber interface.

A mathematical model should also be derived to include surface coatings on composites to determine any potential benefit of these coatings.

Acknowledgement

The authors acknowledge the excellent work done by Mr. H. E. Mathews, Jr. in preparing the composite specimens used in this investigation.

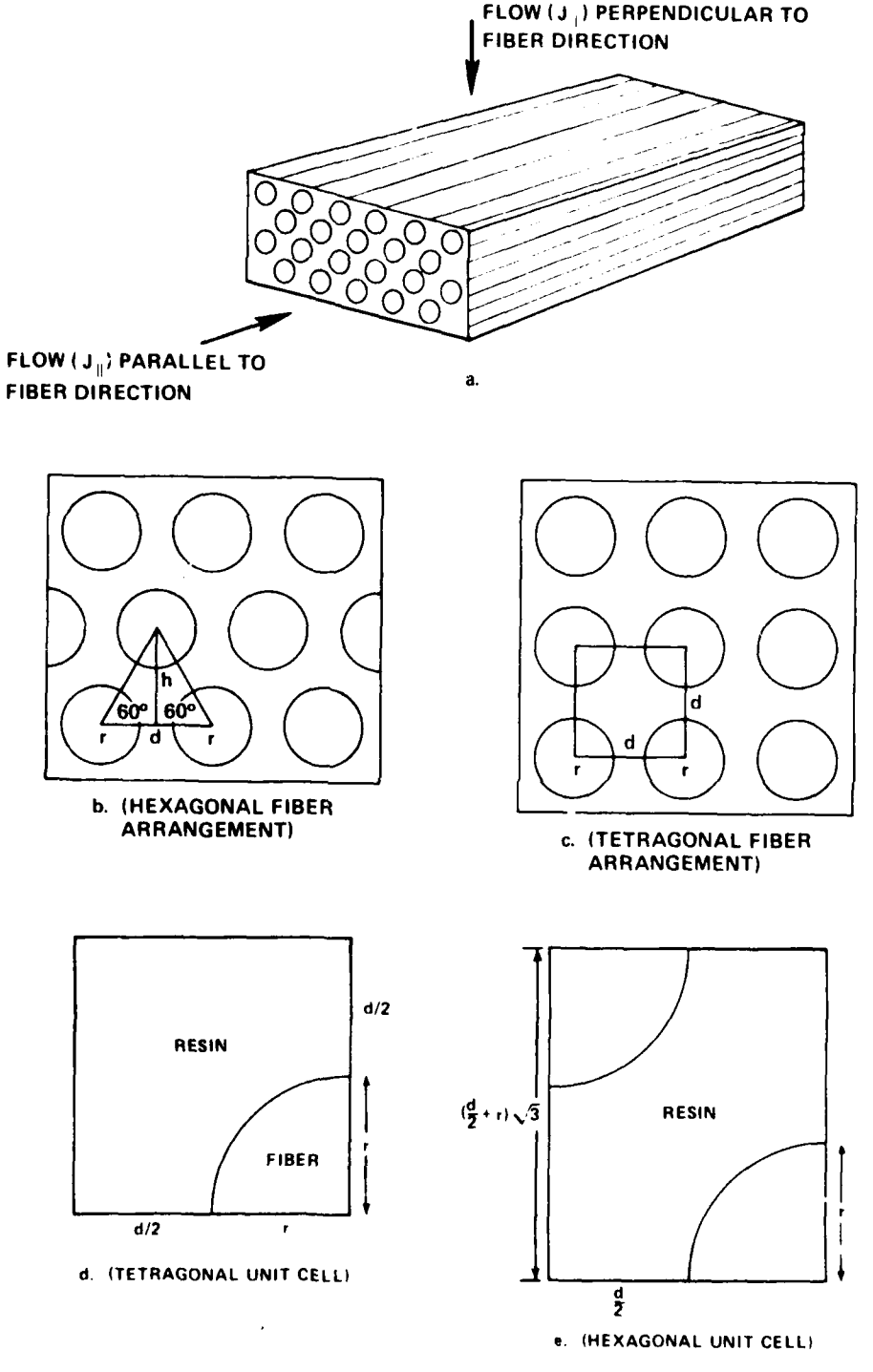


FIG. 1 GEOMETRY OF UNIDIRECTIONAL FIBER REINFORCED COMPOSITES.

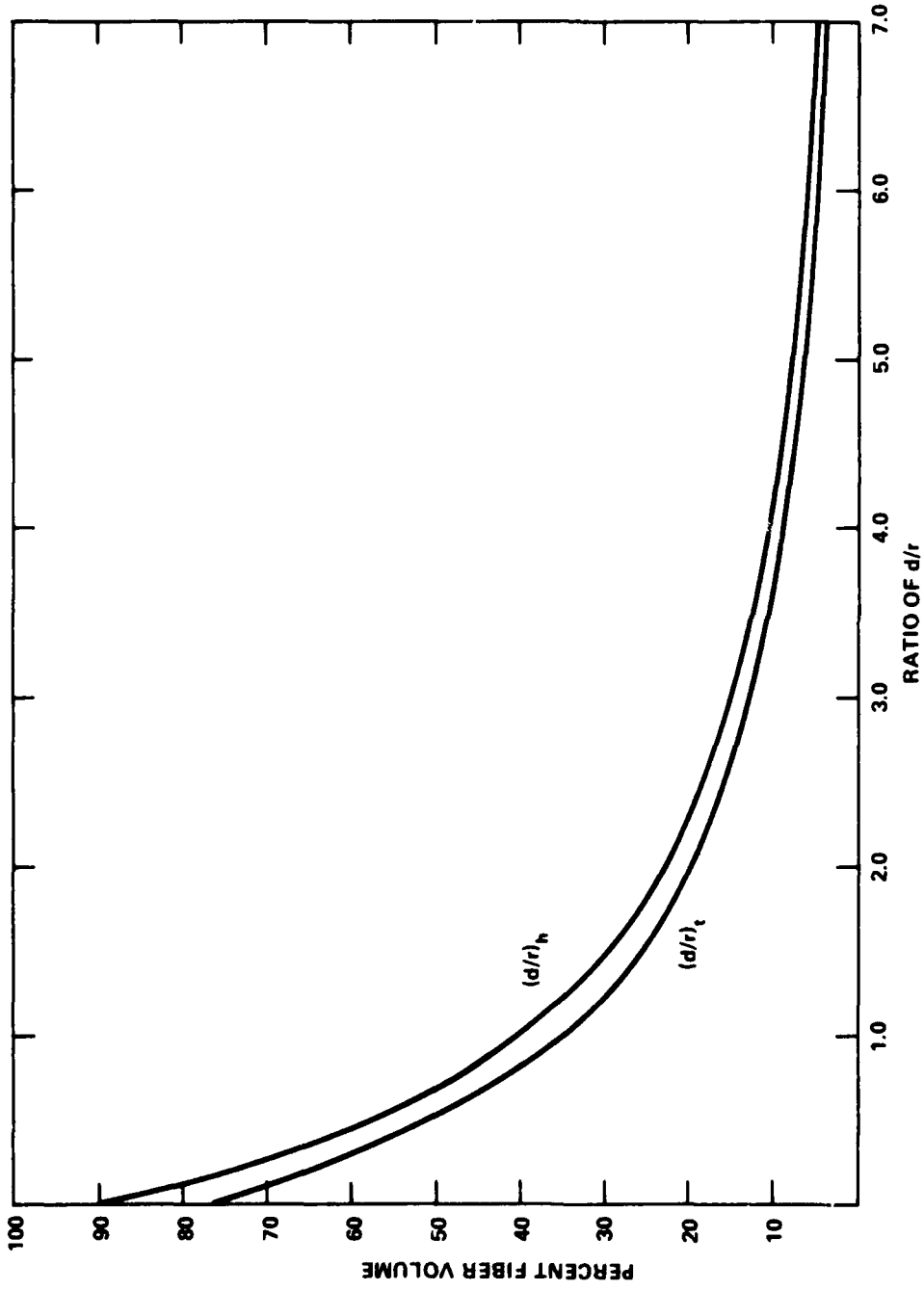


FIG. 2 RELATION OF PERCENT FIBER VOLUME TO THE RATIO OF FIBER DISTANCE TO FIBER RADIUS IN A HEXAGONAL TWO-DIMENSIONAL LATICE OF FIBERS IN A UNIDIRECTIONAL FIBER REINFORCED COMPOSITE (SUBSCRIPT h AND t INDICATE HEXAGONAL AND TETRAGONAL FIBER ARRANGEMENT).

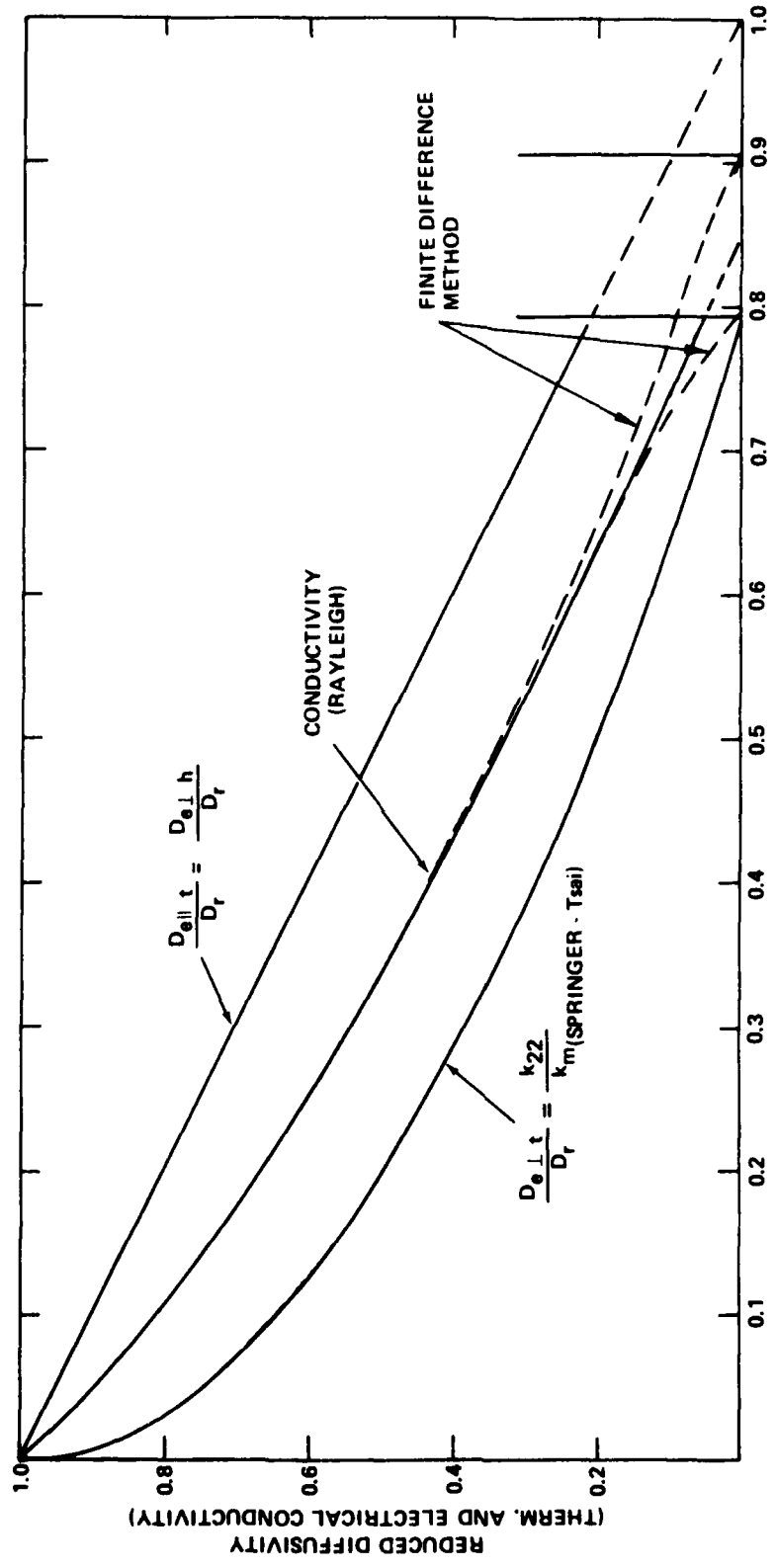


FIG. 3 A COMPARISON OF THE REDUCED DIFFUSIVITY VERTICAL TO THE FIBER DIRECTION WITH THERMAL AND ELECTRICAL ANALOGS.

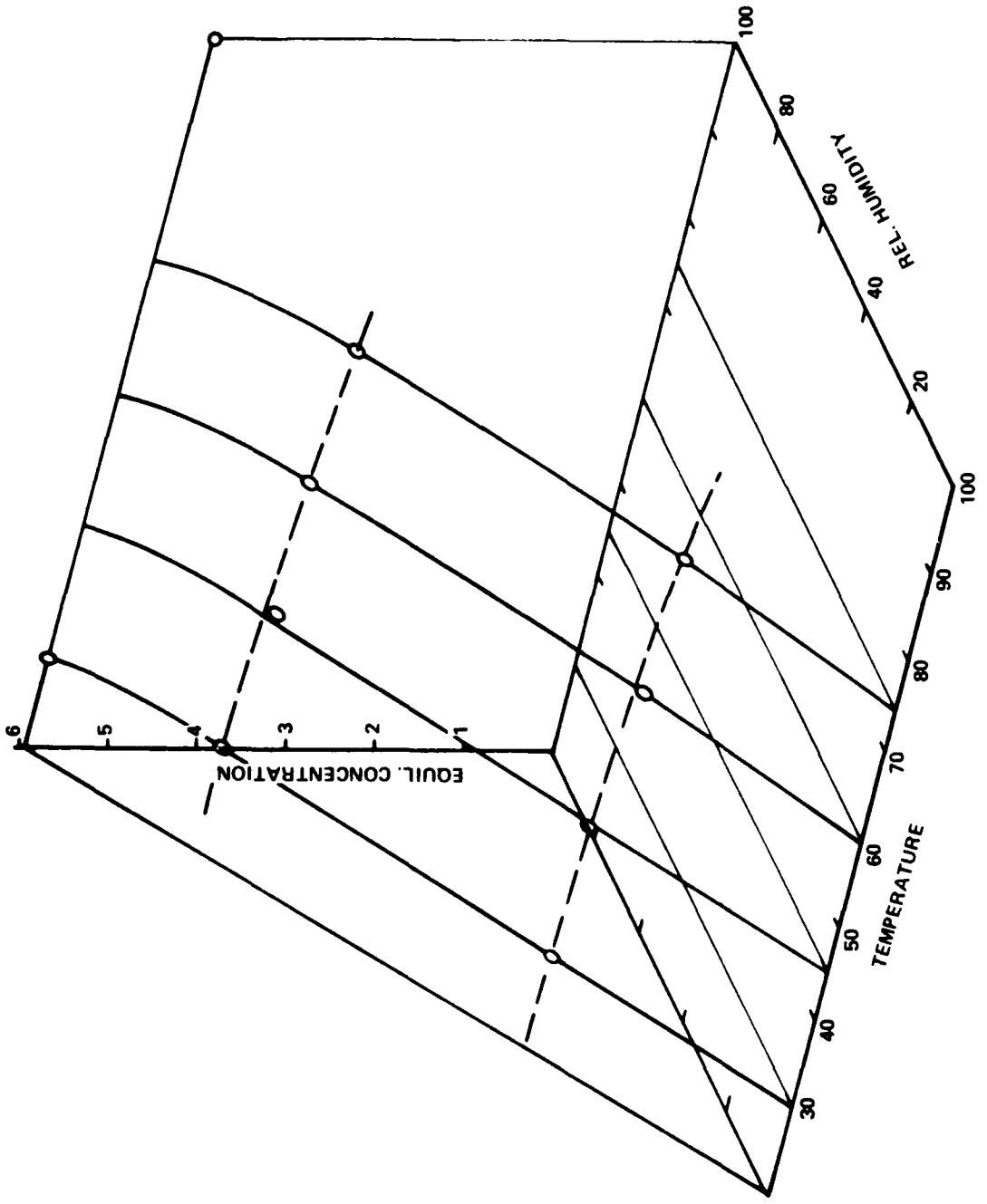


FIG. 4 EQUILIBRIUM CONCENTRATION OF MOISTURE IN NARMCO 5208 RESIN AS A FUNCTION OF TEMPERATURE AND RELATIVE HUMIDITY

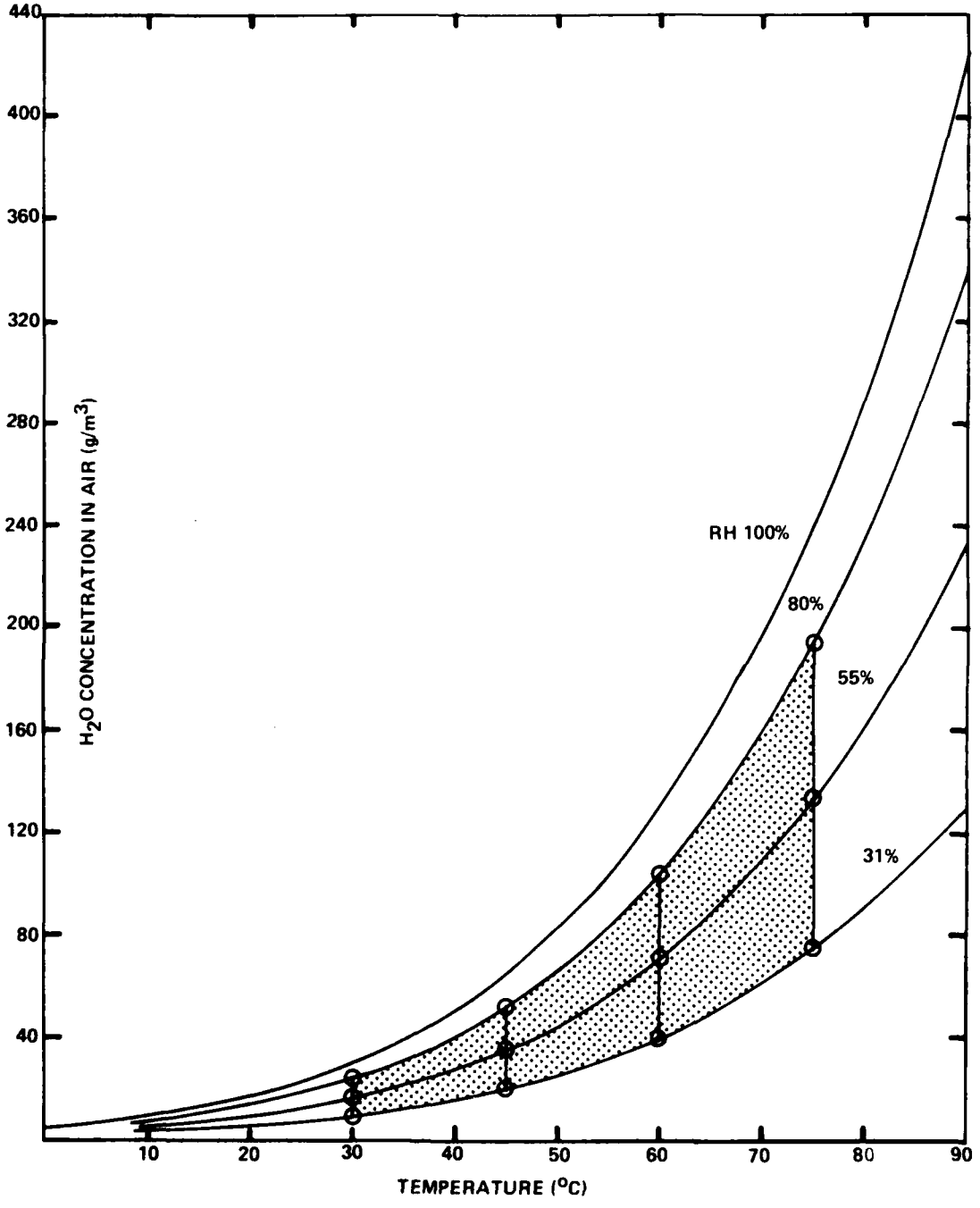


FIG. 5 CONCENTRATION OF MOISTURE IN AIR AS FUNCTION OF TEMPERATURE

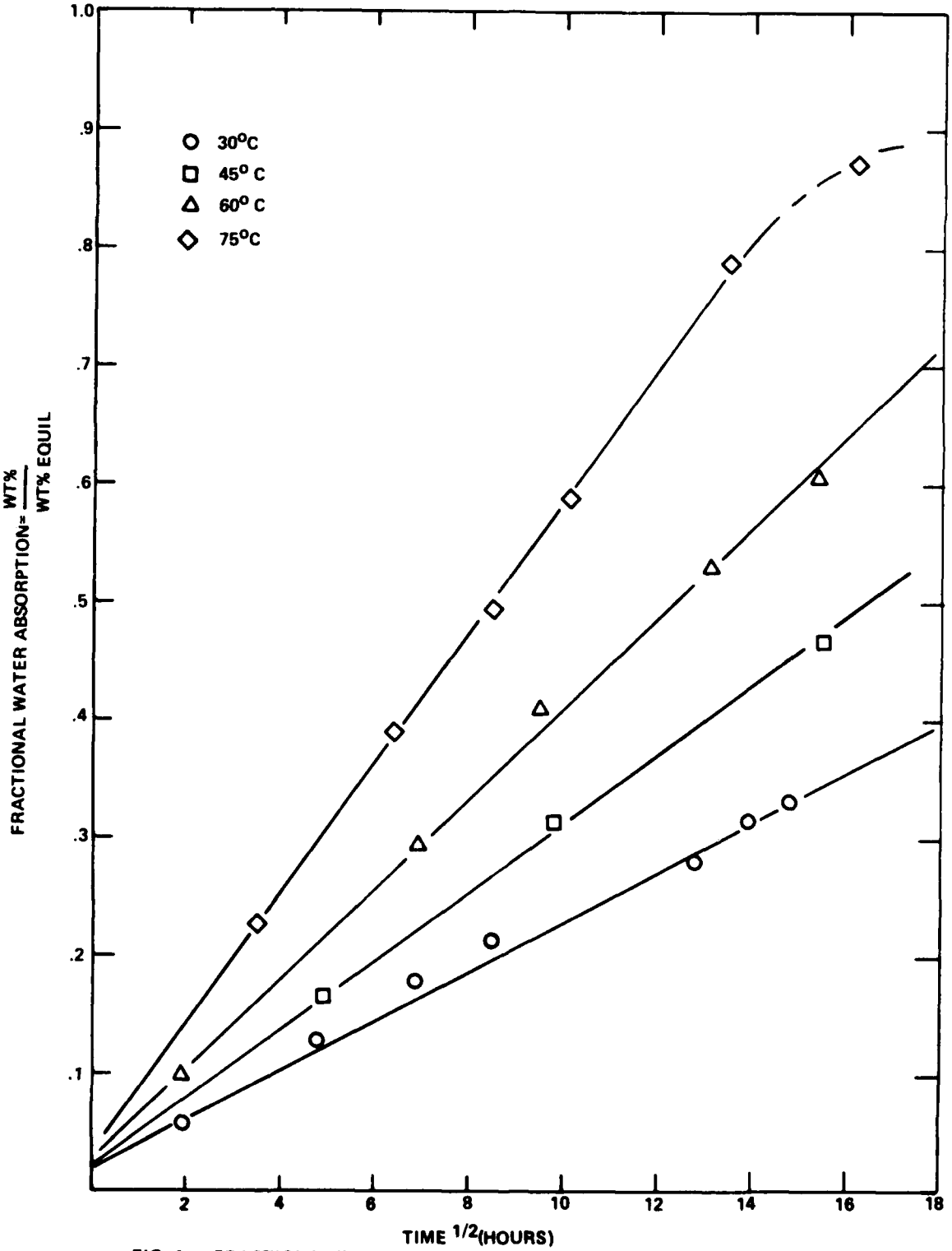


FIG. 6 FRACTIONAL WATER ABSORPTION AT VARIOUS TEMPERATURES OF EPON 1031/HMS COMPOSITE AT 30% RH

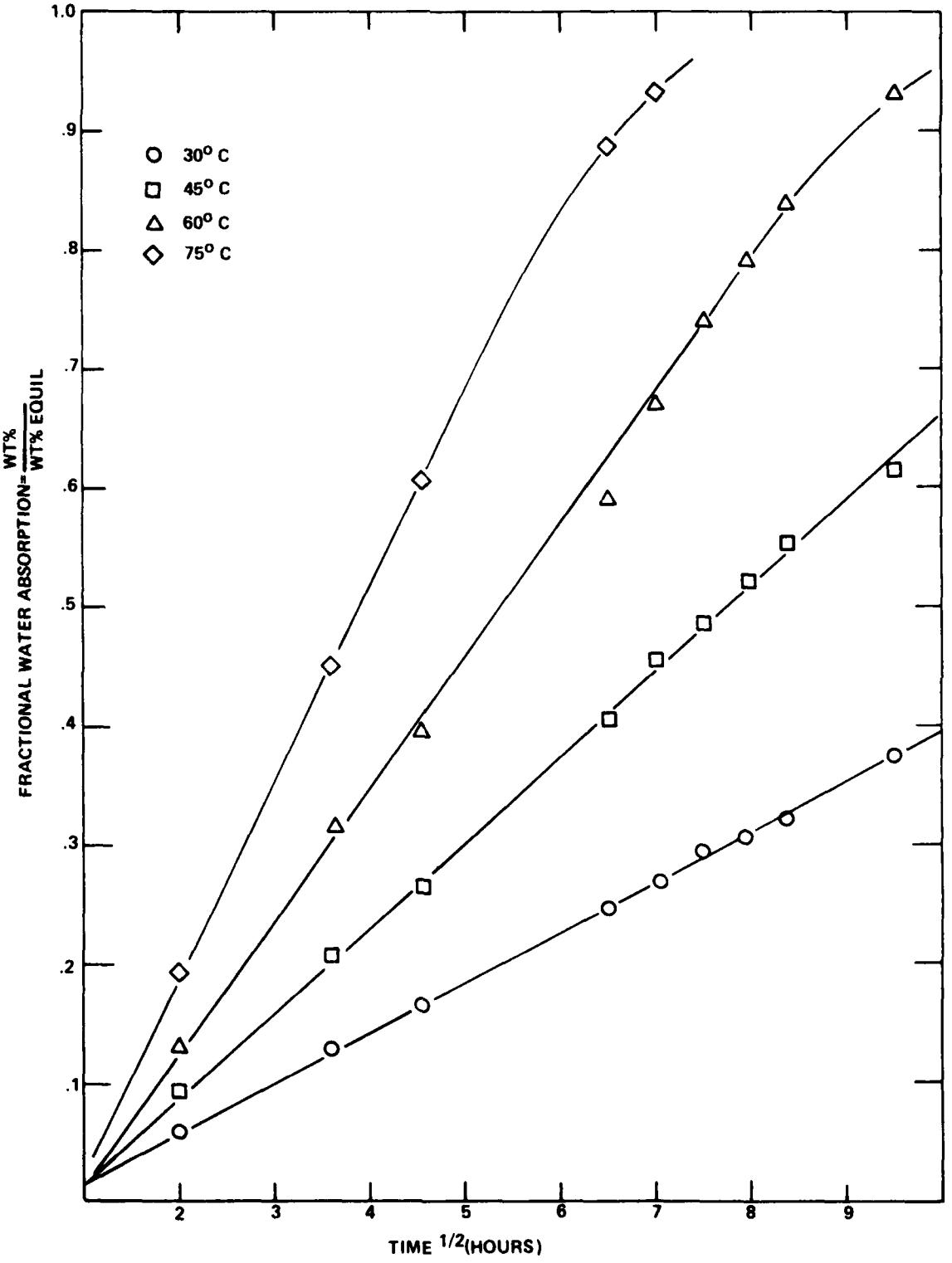


FIG. 7 FRACTIONAL WATER ABSORPTION AT VARIOUS TEMPERATURES OF EPON 1031/HMS COMPOSITE AT 80% RH

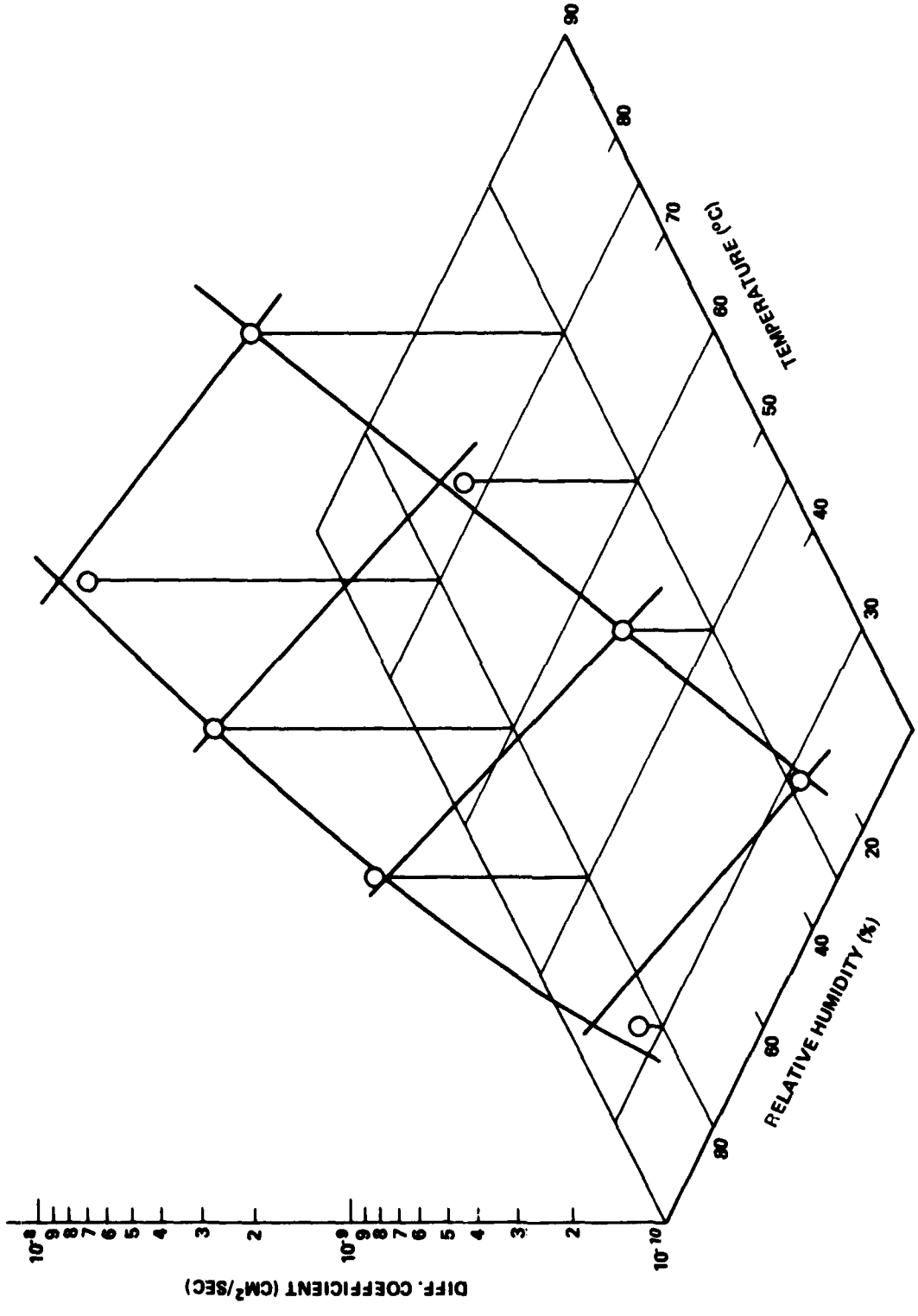


FIG. 8 DIFF. COEFFICIENT OF WATER FOR NARMCO 5208/T300 C-FIBER COMPOSITE AS A FUNCTION OF TEMP. AND REL. HUMIDITY

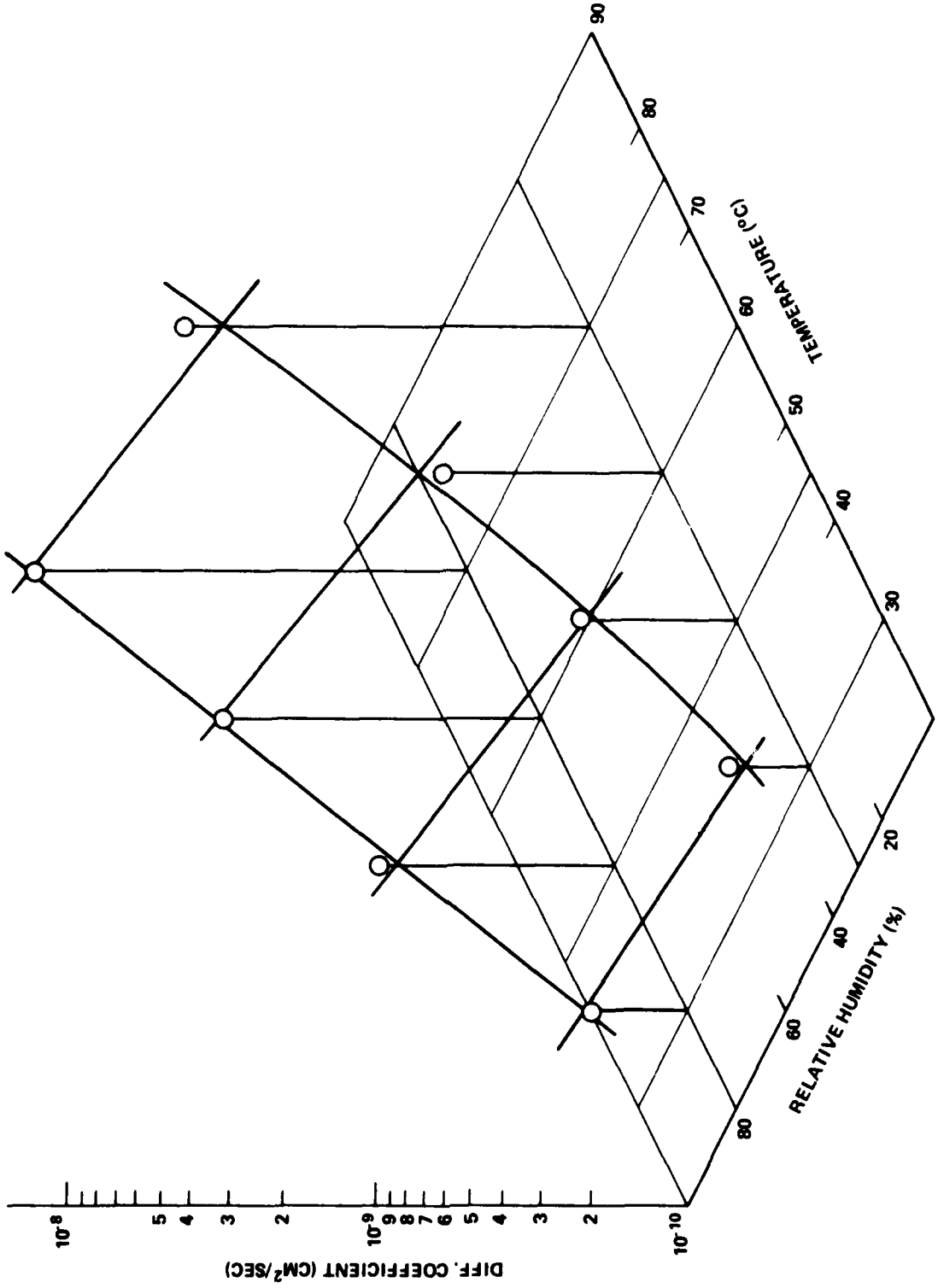


FIG. 9 DIFF. COEFFICIENT OF WATER FOR DER 332/T300 C-FIBER COMPOSITE AS A FUNCTION OF TEMP. AND REL. HUMIDITY

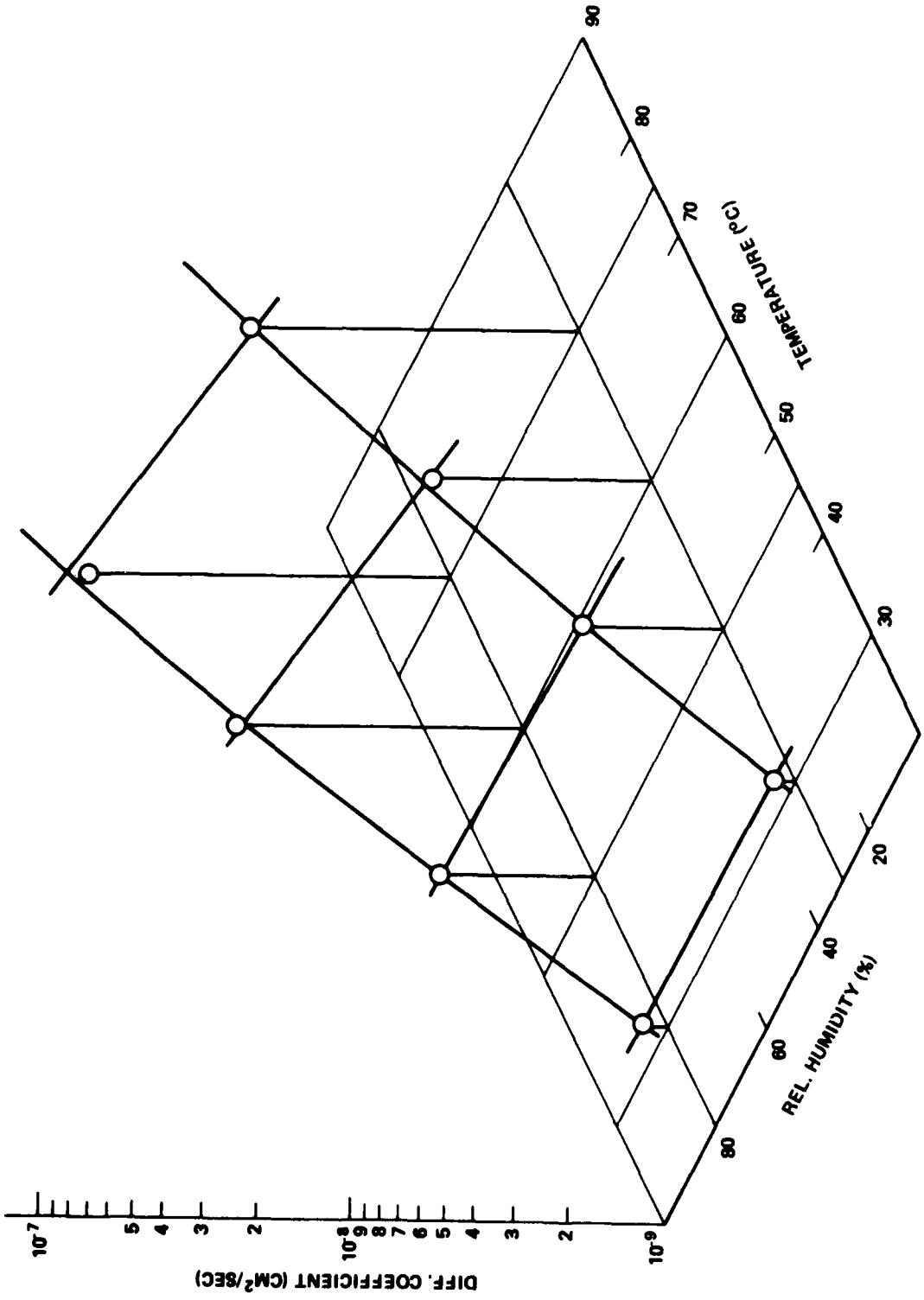


FIG. 10 DIFF. COEFFICIENT OF WATER FOR EPON 1031-T300 C-FIBER COMPOSITE AS A FUNCTION OF TEMP. AND REL. HUMIDITY

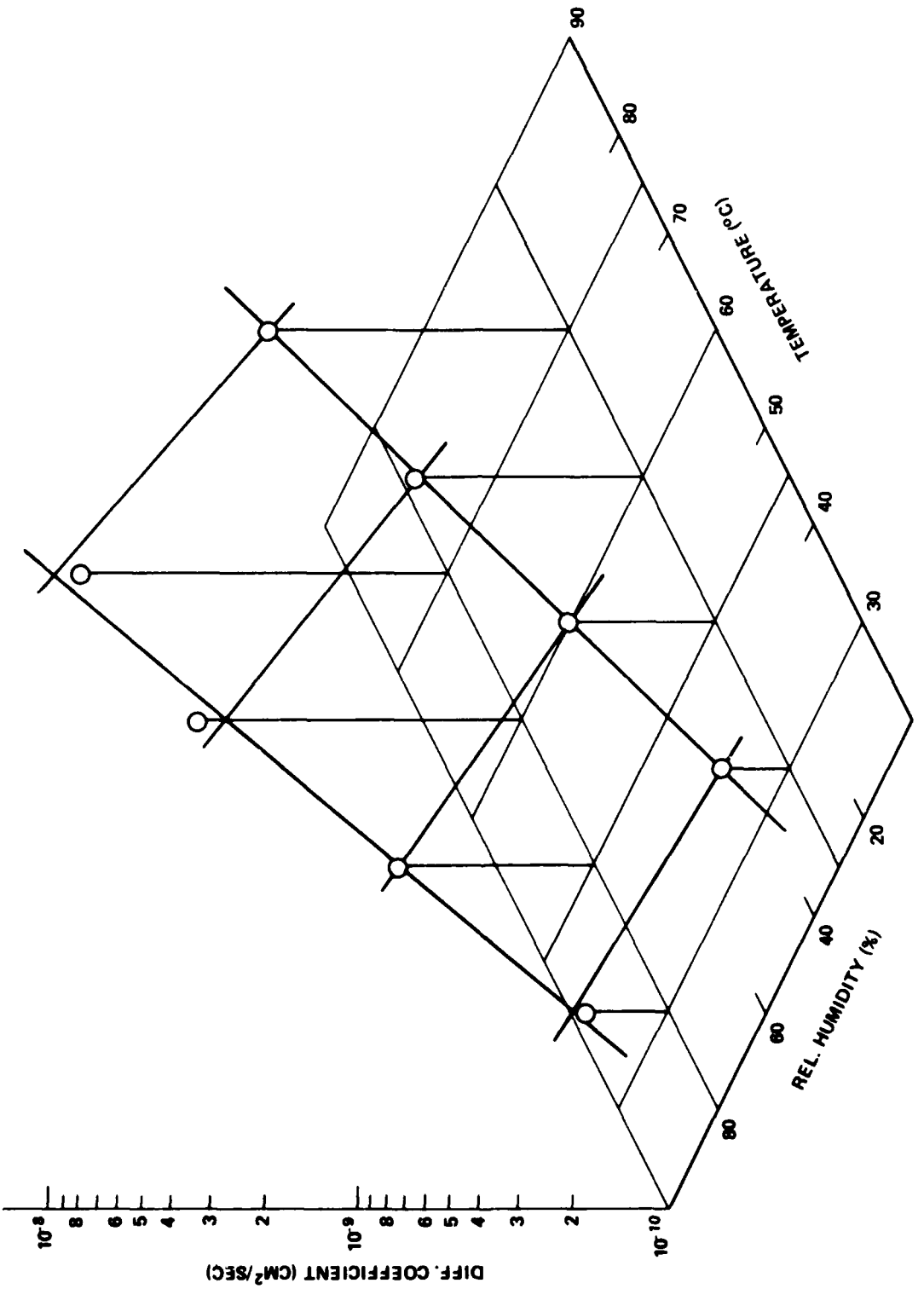


FIG. 11 DIFF. COEFFICIENT OF WATER FOR NARMCO 5208/HMS C-FIBER COMPOSITE AS A FUNCTION OF TEMP. AND REL. HUMIDITY

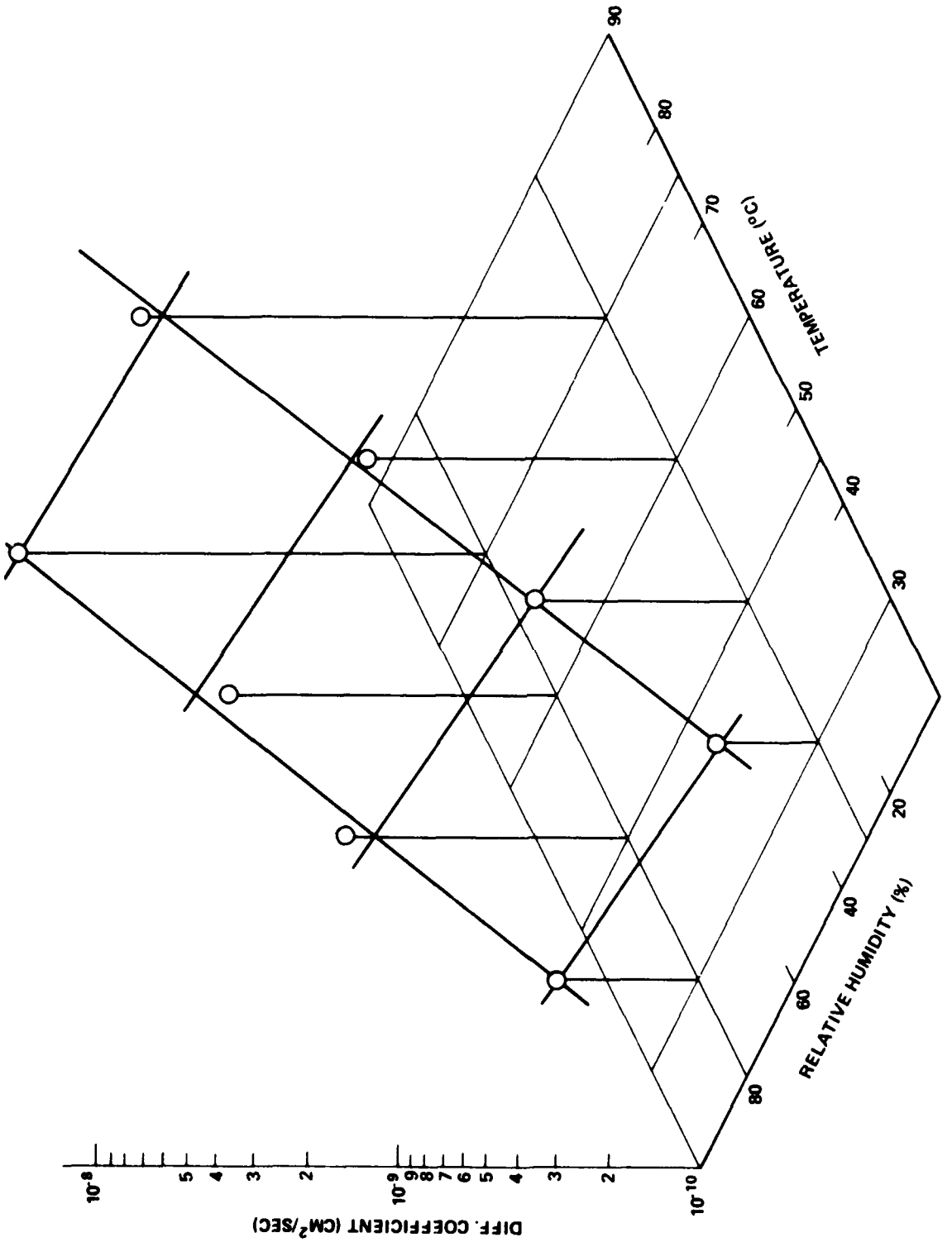


FIG. 12 DIFF. COEFFICIENT OF WATER FOR DER 332/HMS C-FIBER COMPOSITE AS A FUNCTION OF TEMP. AND REL. HUMIDITY

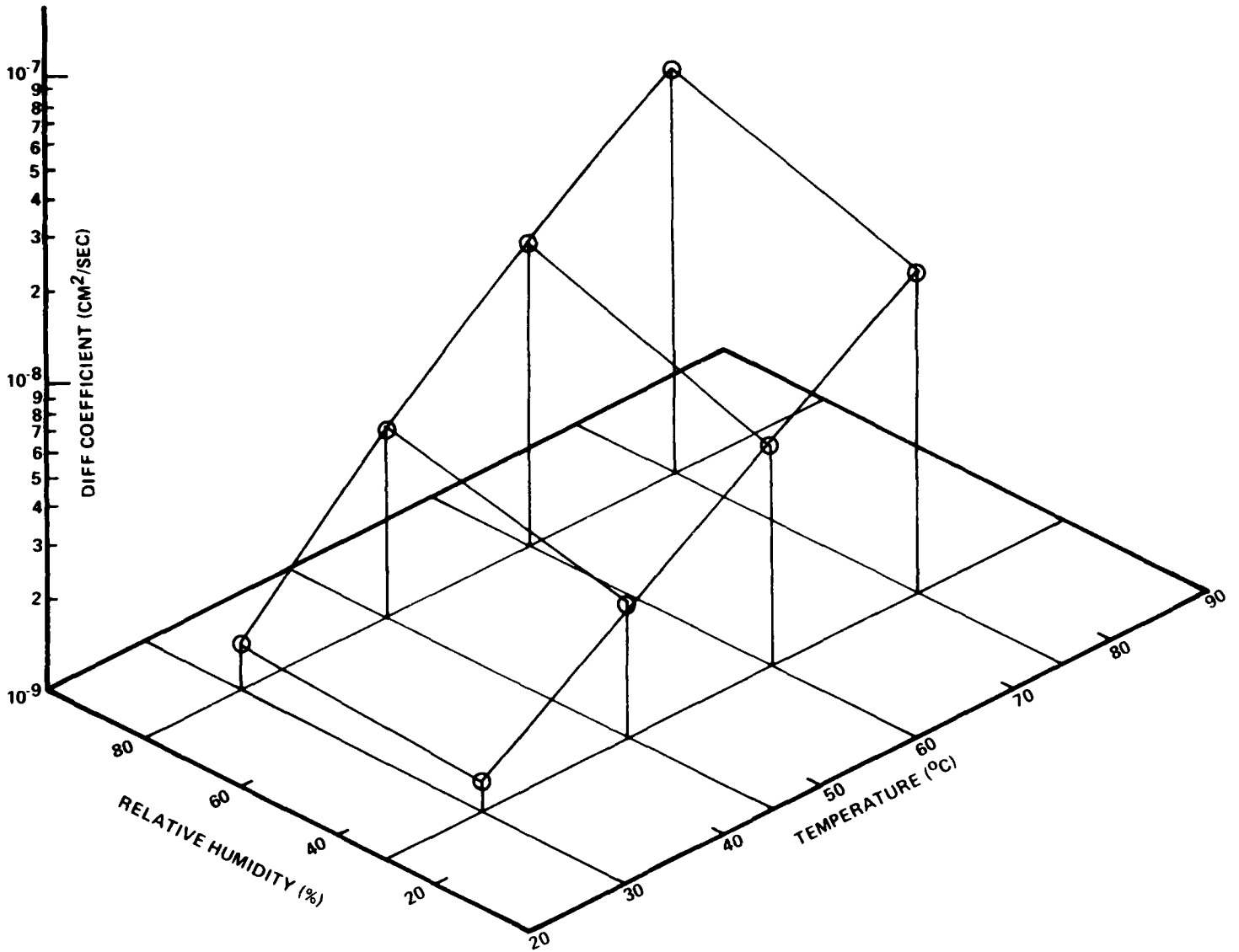


FIG. 13 DIFFUSION COEFFICIENT OF WATER FOR EPON 1031-HMS COMPOSITE AS A FUNCTION OF TEMPERATURE AND RELATIVE HUMIDITY

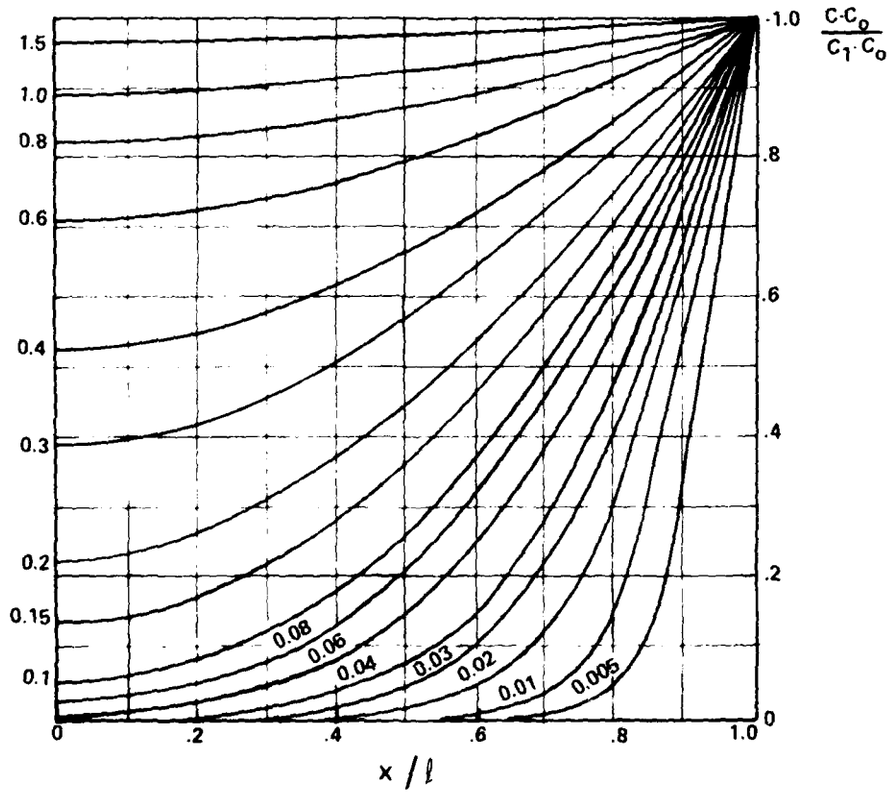


FIG. 14 CONCENTRATION DISTRIBUTION (MASTER PLOT) AT VARIOUS TIMES IN THE SHEET $-h < X < h$ WITH INITIAL UNIFORM CONCENTRATION $C_o$ AND SURFACE CONCENTRATION $C_1$. NUMBERS ON CURVES ARE VALVES OF $Dt/h^2$.

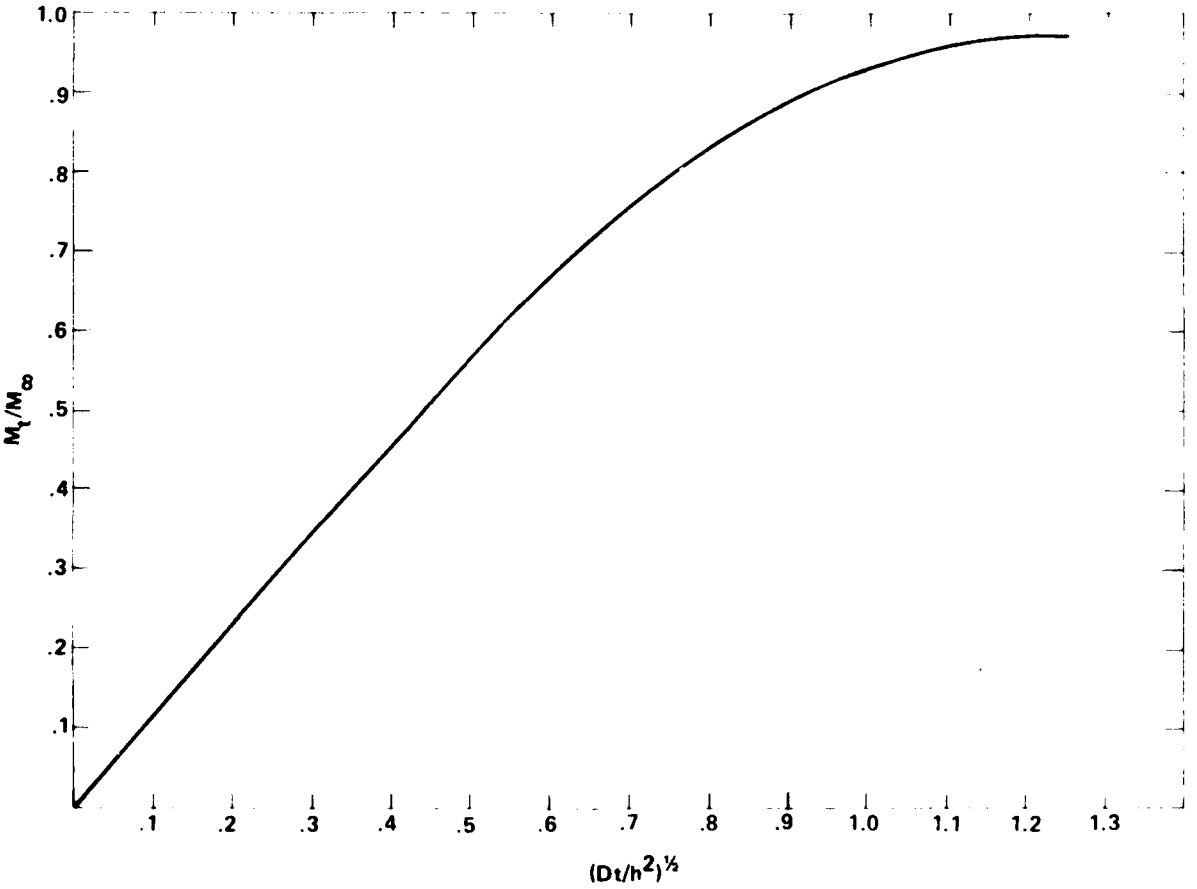


FIG. 15 PLOT OF FRACTIONAL ABSORPTION OF ANY MATERIAL WITH FICKEAN BEHAVIOR VERSUS $(Dt/h^2)^{1/2}$ FOR PLATE GEOMETRY

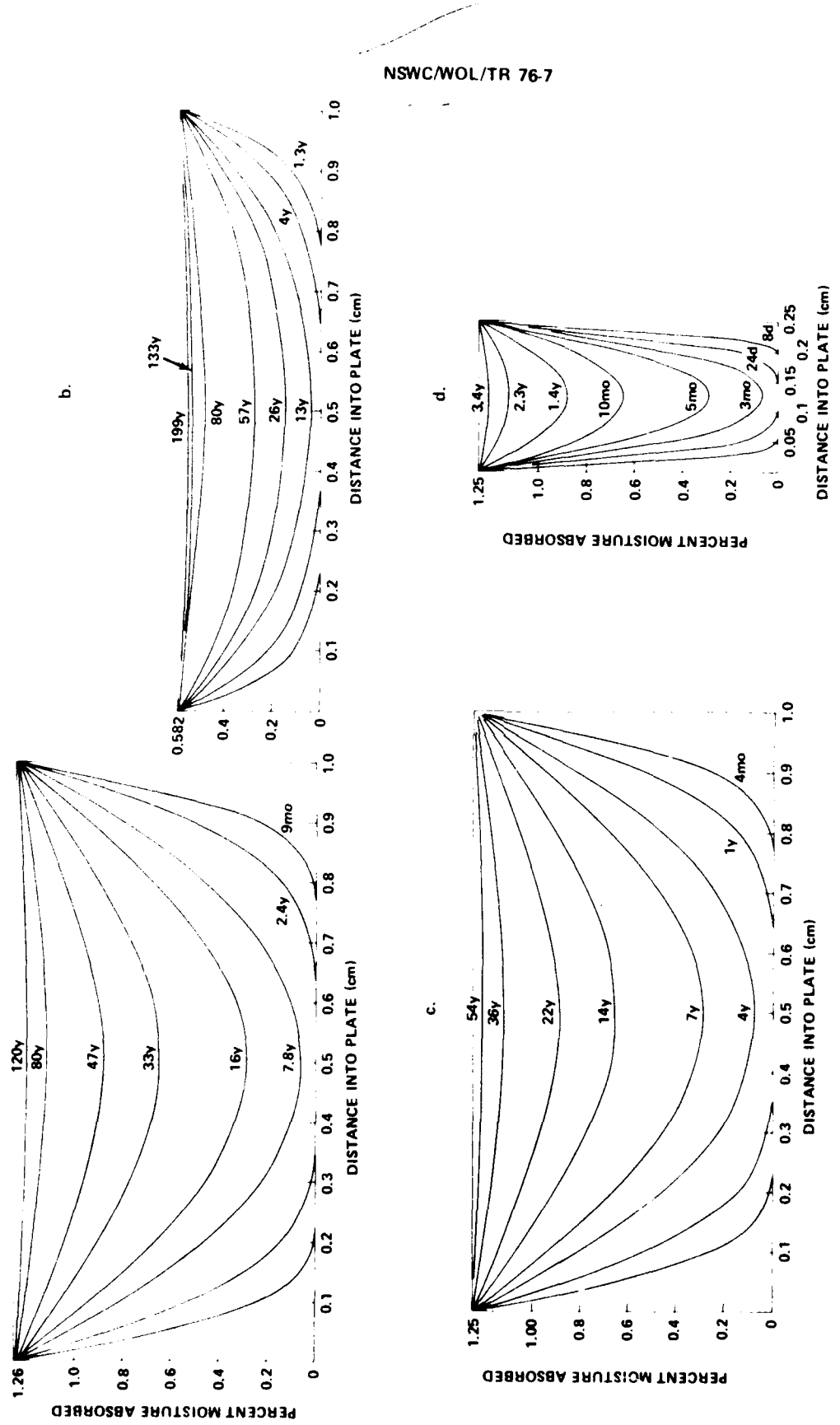


FIG. 16 DISTRIBUTION OF MOISTURE IN A UNIDIRECTIONAL 5208/T300 EPOXY COMPOSITE:
a. AT 25°C AND 80% RH (THICKNESS 1 CM); b. AT 25°C AND 30% RH (THICKNESS 1CM);
c. AT 35°C AND 80% RH; d. AT 36°C AND 80% RH (THICKNESS 0.25 CM)

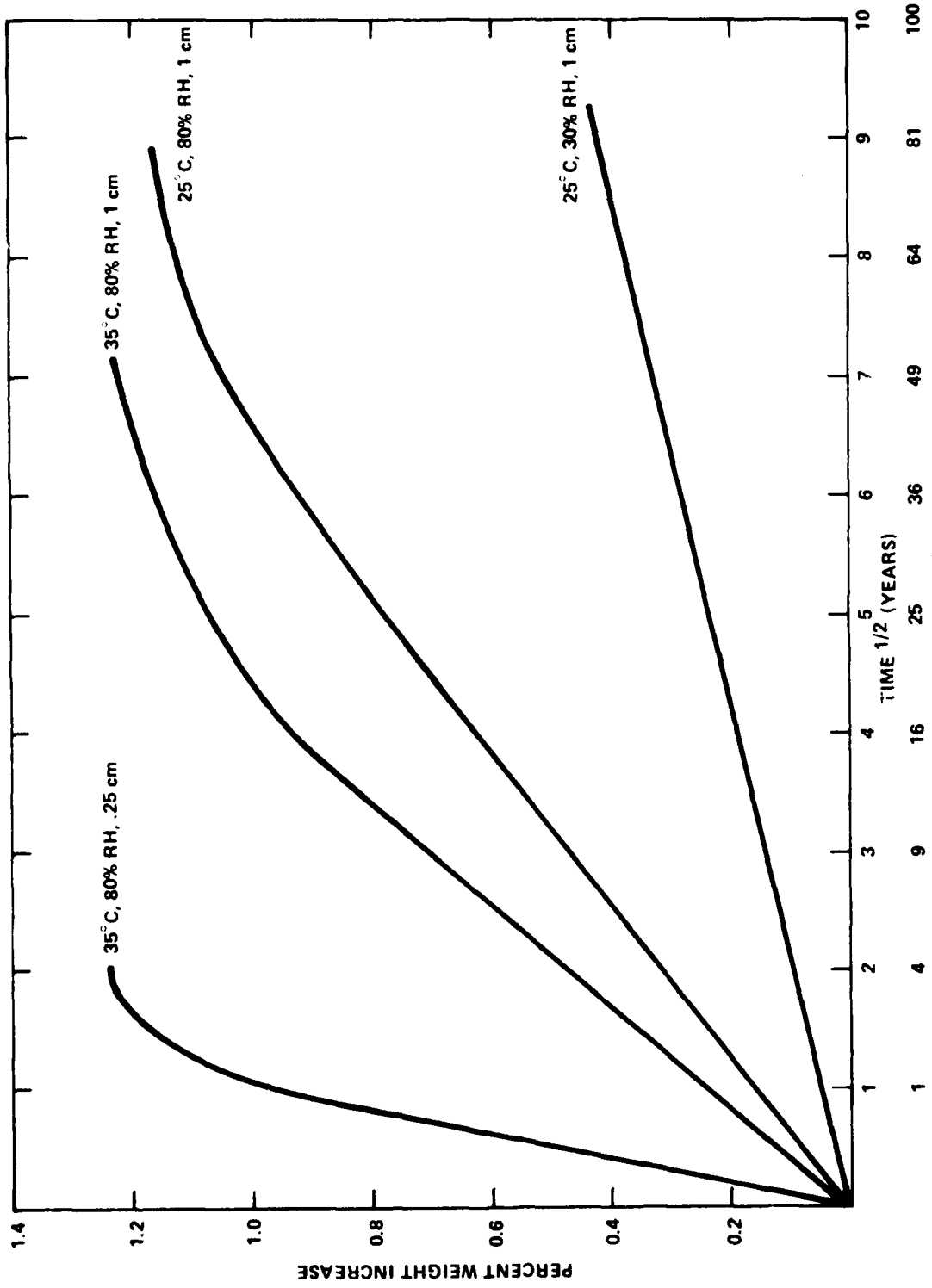


FIG. 17 PERCENT WEIGHT INCREASE OF 5208/T300 EPOXY COMPOSITE AT VARIOUS CONDITIONS. (THE FIRST NUMBER INDICATES EXPOSURE TEMPERATURE, THE SECOND INDICATES % REL. HUMIDITY, THE THIRD INDICATES SPECIMEN THICKNESS)

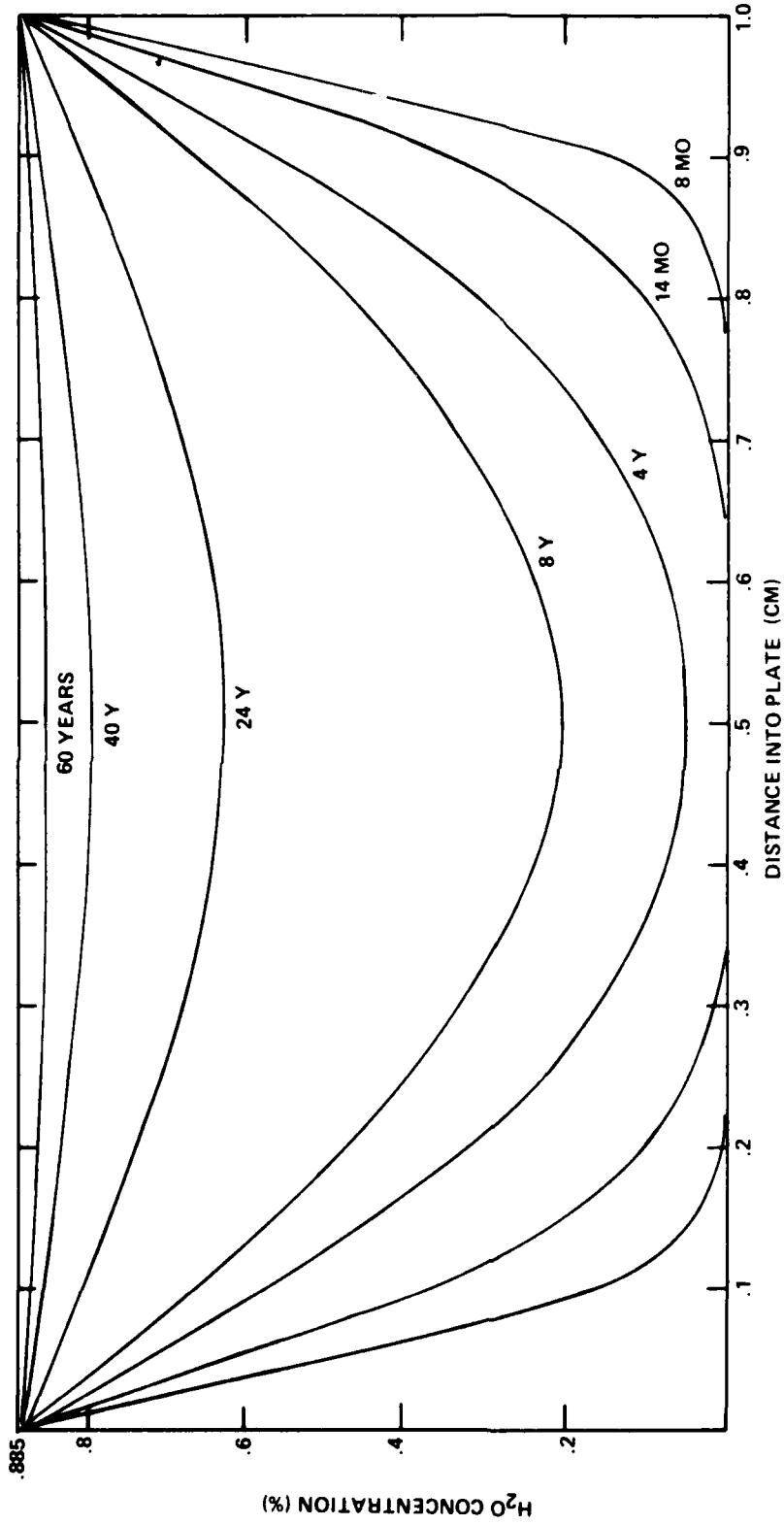


FIG. 18 DIFFUSION OF $H_2O$ INTO DER 332/DADS-HMS COMPOSITE (VERTICAL TO FIBER DIRECTION) AT 25° C AND 80% RH ($D=2X10^{-10}$ $CM^2/SEC$)

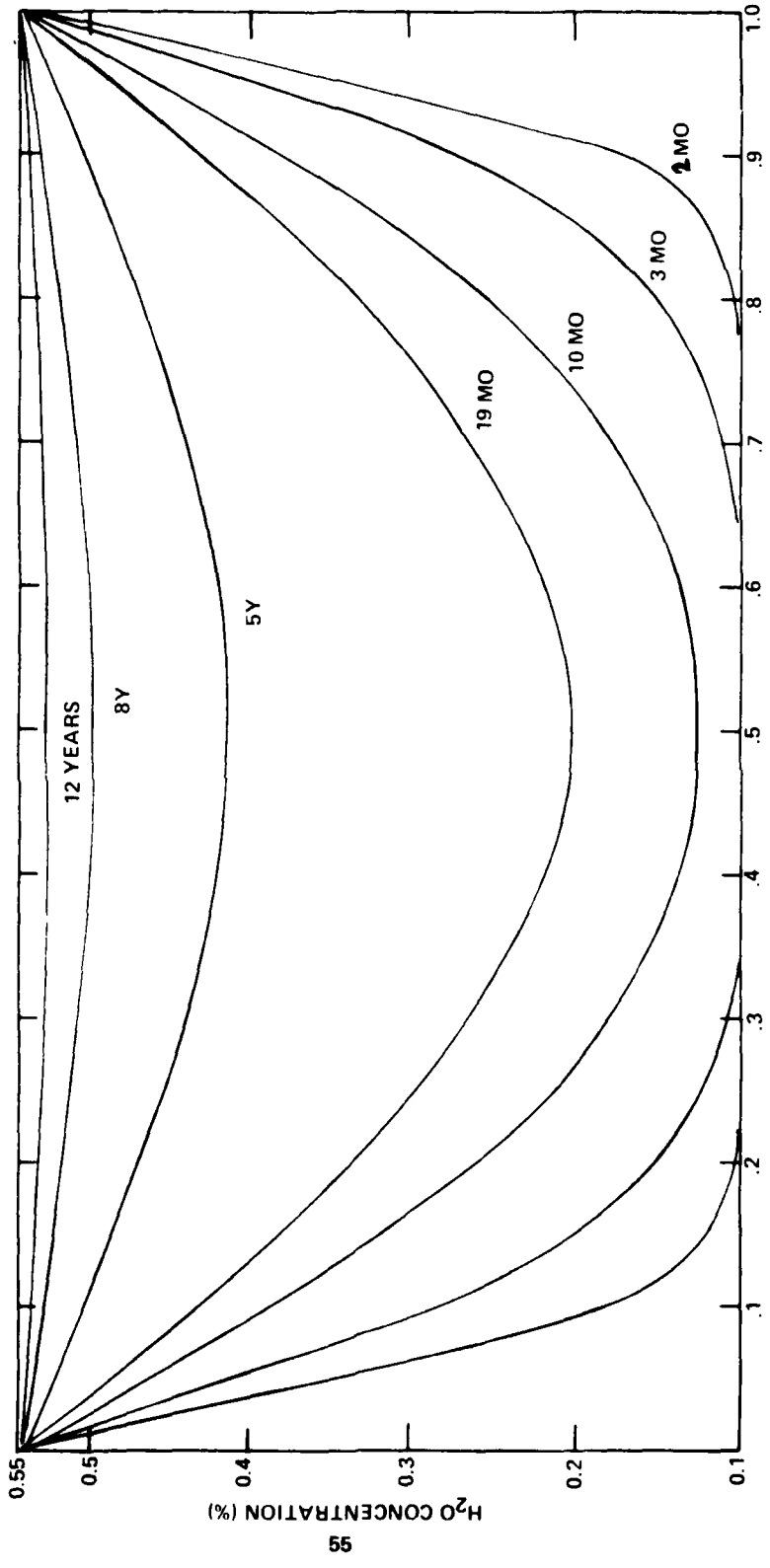


FIG. 19 DIFFUSION OF $H_2O$ INTO EPON 1031/NMA-HMS COMPOSITE (VERTICAL TO FIBER DIRECTION) AT 25° C AND 80% RH ($D=10^{-9}CM^2/SEC$)

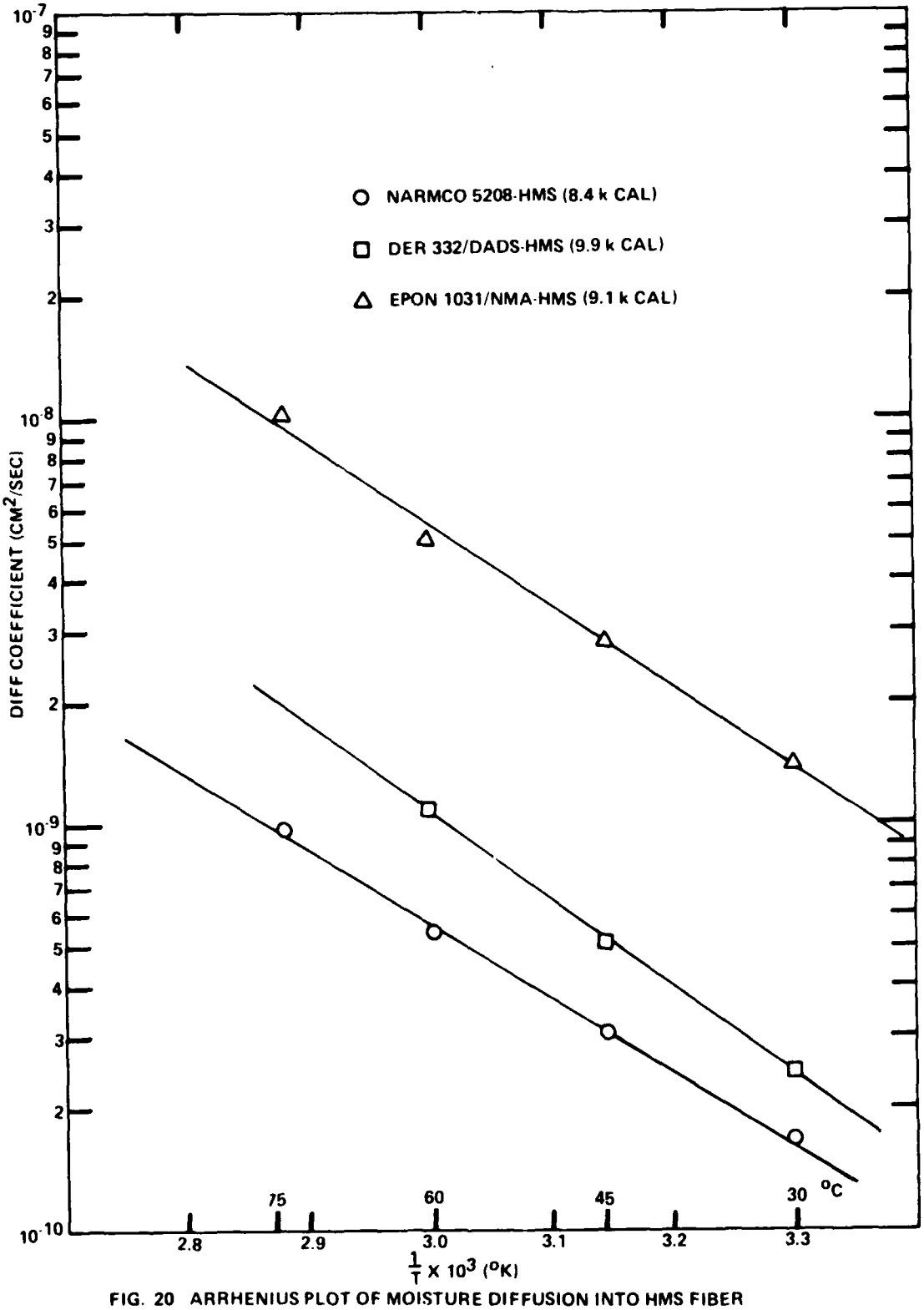


FIG. 20 ARRHENIUS PLOT OF MOISTURE DIFFUSION INTO HMS FIBER COMPOSITES (DETERMINED AT 33% RH

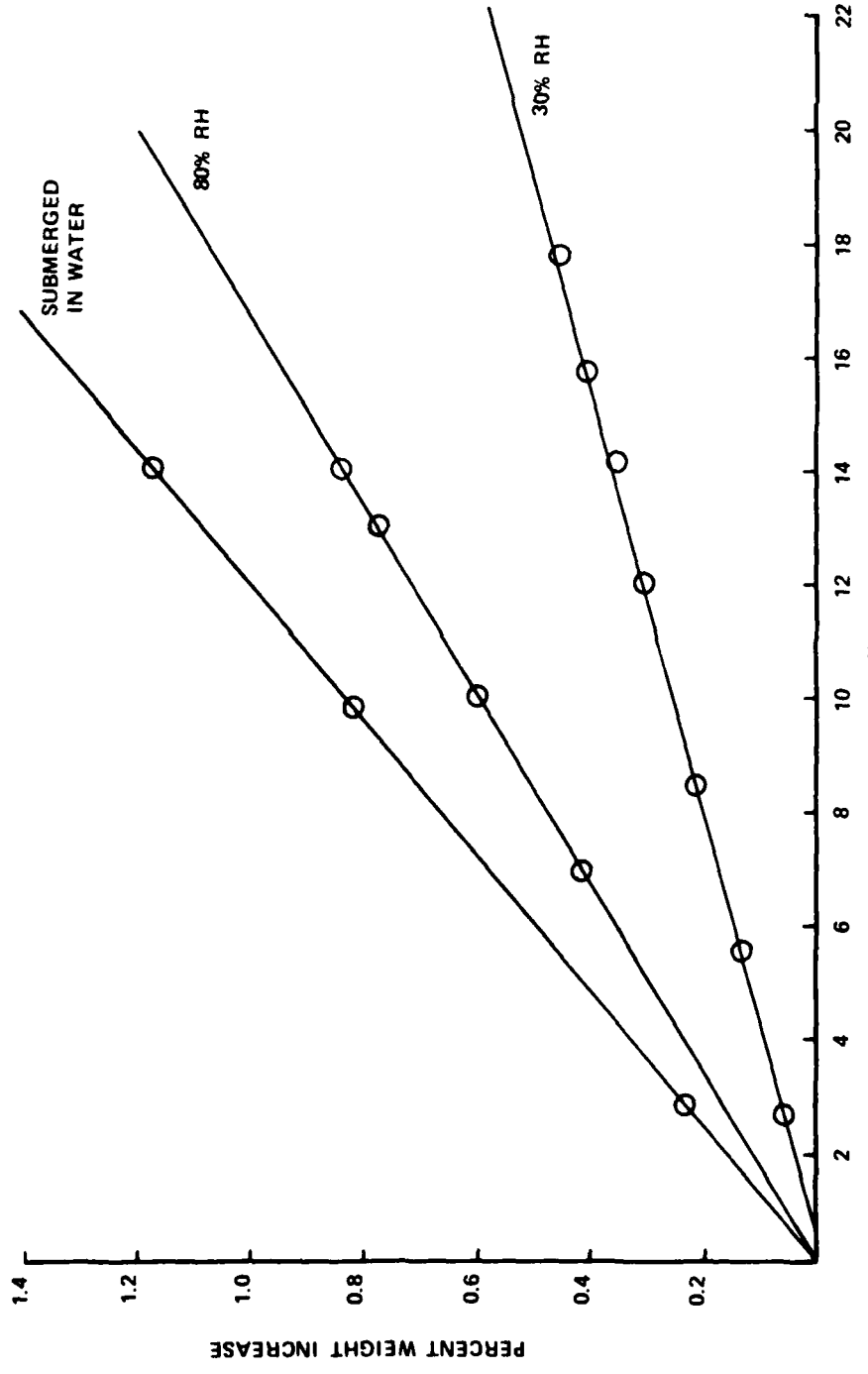


FIG. 21 RATE OF MOISTURE PICK UP IN A 0.370 CM THICK SHEET OF NARMCO 5208 RESIN AT 30° C

# APPENDIX A

## ALGORITHM FOR THE NUMERICAL CALCULATION OF EFFECTIVE DIFFUSION COEFFICIENTS

In this appendix a complete description will be given for the numerical method used to calculate effective diffusion coefficients perpendicular to the fiber direction in a carbon fiber composite. As described in Section E. of Discussion and Results, the geometry under consideration is either hexagonal or tetragonal arrangement of the fibers (Figure 1).

We first demonstrate that it suffices to solve the diffusion problem within a unit cell, and then we give a detailed description of the finite difference method used in solving (24-26).

### A1. Sufficiency of Solving within the Unit Cell

It suffices to show that the solution on the full infinite plate region of the problem can be generated from the solution on the unit cell, and that (as will be obvious from the construction) the effective diffusion coefficient calculated from the unit cell is identical with that obtained from the entire domain of the problem.

The "weak" formulation of (22) is (G ≡ unit cell);

$$\int_G (d(x,y)u_x v_x + d(x,y)u_y v_y)dxdy = 0 \qquad (33)$$

for all square integrable test functions v having square integrable first derivative in G (such functions v are said to be in H'(G)) and which vanish on the line segments y=0 and y=$\bar{y}$ for $0<x<r+d/2$. The solution u of (33) is to lie in H'(G) and satisfy ($\bar{2}2\bar{d}$). Because the interface is smooth and meets the boundary of G at right angles, the (unique) solution u of (33) has square integrable second derivatives within the resin and within the fiber and is continuous on G and its boundary [12], [13]. By using Green's formula on (33) to shift derivatives from v onto u, one has (b≡r+d/2,

[12] R. B. Kellogg, "On the Poisson Equation with Intersecting Interfaces, "Applied Analysis, 4, 101, (1975).
[13] D. P. Squire, "On the Existence and Uniqueness of Solutions of the Poisson Interface Problem, "Am. J. Math. 85, 241, (1963).

I ≡ interface curve, n = unit normal to I pointing into the resin);

$$\int_{G-I} d(x,y)\Delta u\cdot v + \int_{y=0}^{\bar{y}} (d(0,y)u_x(0,y)v(0,y) - d(b,y)u_x(b,y)v(b,y)) + \int_I \left(kD_f u_n^f - D_r u_n^r\right) v=0 \tag{34}$$

and by varying v over H'(G) (with v=0 when y=0 and when y=$\bar{y}$) one recovers (22).

Using the weak formulation, one verifies that the solution may be extended horizontally (i.e. parallel to the x-axis) by reflection (as is intuitively obvious from the symmetry conditions (22e)). To extend vertically, we use the Schwarz reflection principle [14]. By addition of a constant, we may take $C_2=0$ in (22d), and define

$$u(x, -y) = -u(x,y) \quad \text{for } 0\leq y\leq \bar{y}, \text{ all } x \tag{35}$$

Similarly one may continue the solution an arbitrary number of cell heights along the y-axis.

A2. The D'Yakonov ADI Method

Equations (24-26) have the form

$$\nabla\cdot A\nabla u \equiv (A(x,y)u_x)_x + (A(x,y)u_y)_y = 0 \tag{36a}$$

on the rectangle $R = \left\{0<x<b, \quad 0<y<\bar{y}\right\}$

$$u(x,o)=C_2 \text{ and } u(x,\bar{y}) = C_1 \quad \text{for } 0<x<b \tag{36b}$$

$$u_x(o,y) = u_x(b,y) = 0 \quad \text{for } 0<y<\bar{y} \tag{36c}$$

[14] P. R. Garabedian, "Partial Differential Equations," John Wiley and Sons, Inc. 1964.

where for (24-26) $A=\tilde{d}$ and $b=r+d/2$. Following [15], we now describe the D'Yakonov ADI (alternating direction implicit) finite difference method as it applies to (36) (i.e. (24-26)).

We consider (36) to be the steady state of the time dependent problem

$$u_t = \nabla \cdot A \nabla u \quad \text{in } R \tag{37a}$$

$$u(x,o,t) = C_2 \text{ and } u(x,\bar{y},t) = C_1 \text{ for } 0<x<b,\ t \geq 0 \tag{37b}$$

$$u_x(0,y,t) = u_x(b,y,t) = 0 \quad \text{for } 0<y<\bar{y},\ t \geq 0 \tag{37c}$$

$$u(x,y,t) = u_o(x,y) \quad \text{in } R \tag{37d}$$

where $u_o$ is given initial data. By choosing $u_o$ and solving (37) one may approach the steady state solution $u(x,y)$ of (36).

To solve (37), a time step $\Delta t$ and positive integers J and K are chosen; the spatial mesh lengths are then defined to be $\Delta x = b/(J-1)$ and $\Delta y = \bar{y}/(K-1)$. An approximate solution $U^n_{j,k}$ of 37 is then obtained (n=1,2,...) where $U^n_{j,k}$ refers to the value of U at time $n \cdot \Delta t_o$ at the spatial mesh point $((j-1)\Delta x,(k-1)\Delta y)$. By definition $U_{j,k} = u_o((j-1)\Delta x,(k-1)\Delta y)$. Let $r_x \equiv \Delta t/\Delta x^2$, $r_y \equiv \Delta t/\Delta y^2$ and use the notation (for any variable H defined at the mesh points)

$$\delta_x A\, \delta_x H_{j,k} \equiv A_{j+1/2,k}\left(H_{j+1,k}-H_{j,k}\right) - A_{j-1/2,k}\left(H_{j,k}-H_{j-1,k}\right)$$

$$\delta_y A\, \delta_y H_{j,k} \equiv A_{j,k+1/2}\left(H_{j,k+1}-H_{j,k}\right) - A_{j,k-1/2}\left(H_{j,k}-H_{j,k-1}\right)$$

where $A_{j+1/2,k} = A((j+1/2)\Delta x, k\Delta y)$ etc.

The D'Yakonov formula (i.e. system of linear equations) for obtaining $U^{n+1}_{j,k}$ from $U^n_{j,k}$ which involves intermediate values $V^{n+1}_{j,k}$ is;

$$\left(1 - \frac{1}{2} r_x \delta_x A \delta_x\right) V^{n+1}_{j,k} = Z^n_{j,k} \text{ for } 1 \leq j \leq J,\ 2 \leq k \leq K-1 \tag{38a}$$

[15] A. R. Mitchell, "Computational Methods in Partial Differential Equations," John Wiley Sons Ltd., 1969.

$$\left(1 - \frac{1}{2}\ r_y\ \delta_y\ A\delta_y\right) U^{n+1}_{j,k} = V^{n+1}_{j,k} \text{ for } 1\le j\le J,\ 2\le k\le k-1 \qquad (38b)$$

where

$$Z^n_{j,k} \equiv (1 + \frac{1}{2}\ r_x\delta_x A\delta_x)(1 + \frac{1}{2}\ r_y\ \delta_y\ A\delta_y)U^n_{j,k} \quad \text{for } 1\le j\le J,\ 2\le k\le K-1 \qquad (39)$$

By making use of the boundary conditions (37b,c) we define

$$U^n_{j,1} = C_2,\ U^n_{j,K} = C_1 \quad \text{for } 0\le j\le J+1,\ n=0,1,2,\ \ldots \qquad (40a)$$

$$U^n_{o,k} = U^n_{2,k},\quad U^n_{J+1,k} = U^n_{J-1,k} \quad \text{for } 1\le k\le K,\ n=0,1,2,\ \ldots \qquad (40b)$$

and (also by symmetry)

$$A_{\frac{1}{2},k} = A_{\frac{3}{2},k},\quad A_{J+\frac{1}{2},k} = A_{J-\frac{1}{2},k} \quad \text{for } 1\le k\le K \qquad (40c)$$

and from (38b)

$$V^n_{o,k} = V^n_{2,k},\ V^n_{J+1,k} = V^n_{J-1,k} \quad \text{for } 2\le k\le K-1, n=1,2,\ \ldots \qquad (40d)$$

which completes the Equations (38). The point of the ADI method is that (38a) involves K-2 separate tridiagonal linear systems of J equations, rather than a total system of J(K-2) linear equations (and similarly with (38b)) which results in a drastic decrease in the work necessary to solve the equations.

## A3. Comments on Implementation

Concerning actual computer implementation of the D'Yakonov method, the following observations are useful. Since the coefficient A and the boundary conditions in (37) are independent of time, the decomposition of the K-2 tridiagonal linear systems from (38a) (and the J systems from (38b)) can be done once and then stored. Letting

$$Q_{j,k} \equiv (1 + \frac{1}{2}\ r_y\ \delta_y\ A\ \delta_y)\ U^o_{j,k} \quad \text{for } 0\le j\le J+1,\ 2\le k\le K-1$$

so

$$Z^{o}_{j,k} = (1 + \frac{1}{2} r_x \delta_x A\delta_x) Q_{j,k} \quad \text{for } 1 \leq j \leq J,\ 2 \leq k \leq k-1$$

one notes by using the boundary conditions (37b,c) which gave (40) that

$$Q_{o,k} = Q_{2,k},\ Q_{J+1,k} = Q_{J-1,k} \quad \text{for } 2 \leq k \leq K-1. \tag{41}$$

It is also very useful to note the following method for calculating $Z^n$ (n=1,2,...) [16], [17]. Suppose we have just calculated $U^n_{j,k}$. We then have available (assuming proper strategy in the computer code). $U^n_{j,k}$, $V^n_{j,k}$, and $Z^{n-1}_{j,k}$. We observe that from (38b) (and dropping the subscripts j,k)

$$U^n - V^n = \frac{1}{2} r_y \delta_y A\delta_y U^n$$

from which

$$(1 + \frac{1}{2} r_y \delta_y A\delta_y) U^n = 2U^n - V^n$$

so

$$Z^n = (1 + \frac{1}{2} r_x \delta_x A\delta_x)(2U^n - V^n)$$

but by (38a)

$$(1 - \frac{1}{2} r_x \delta_x A\delta_x) V^n = Z^{n-1}$$

from which

$$-\frac{1}{2} r_x \delta_x A\delta_x V^n = Z^{n-1} - V^n$$

[16] S. Leventhal, personal communication
[17] M. Ciment and S. Leventhal, "Higher Order Compact Implicit Schemes for the Wave Equation," Math. Comp., 29, 985, (1975).

and so

$$z^n = 2U^n - V^n + \frac{1}{2}r_x\delta_x A\delta_x\, 2U^n + z^{n-1} - V^n, \text{ and}$$

$$z^n = 2U^n - 2V^n + z^{n-1} + r_x\delta_x A\delta_x\, U^n \tag{42}$$

which greatly simplifies the computation of $z^n$ at each step.

A4. Calculation of Diffusion Coefficients

The D'Yakonov ADI scheme was used to solve (24-26) by relaxing the corresponding time dependent problem toward the steady state. Then $d_e$ was obtained using (19) and

$$q = \int_0^{r+d/2} - \tilde{d}(x,y)\, U_y\,(x,y)dx \quad \text{for any } y\varepsilon\,[o,\bar{y}]. \tag{43}$$

Since actually it is the ratio $d_e/D_r$ that is of interest, we may scale distance so that b=1 and time so that $D_r$=1. For convenience we also set $C_1$=0 and $C_2=\bar{y}$ so that (from (19)) $d_e/D_r = q$.

The explicit definition of $\tilde{d}(x,y)$ for the tetragonal unit cell is as follows. A parameter z>0 is given (in general we took z = .02 with J=K=21). Given (x,y), let $\rho = ((x-b)^2 + y^2)^{1/2}$ and define $\bar{D}_f = \max(.001, D_f)$. If $\rho \geq r + z$, then $\tilde{d}(x,y) = D_r$; while if $\rho \leq r-z$, then $\tilde{d}(x,y) = \bar{D}_f \cdot k$. For $r-z \leq \rho \leq r+z$,

$$\tilde{d}(x,y) = \bar{D}_f \cdot k + (\rho-(r-z))(D_r - \bar{D}_f\, k)/(2z).$$

For the hexagonal unit cell one also similarly deals with the fiber centered at $(0,\bar{y})$. In the hexagonal case we generally choose z=.02 with J=21 and K=41.

The calculation of (43) was done at several different $y_m$ values ($y_m \equiv (m - 1/2)\Delta y$) using the trapezoidal rule;

$$q \approx q_m^n = \sum_{i=1}^{J-1} -\Delta x \left[\tilde{d}((i-1)\Delta x, y_m)(U^n_{i-1,\,m+1} - U^n_{i-1,m}) + d(i\Delta x, y_m)(U^n_{i,m+1} - U^n_{i,m})\right] \Big/ 2\Delta y \tag{44}$$

Comparing $q_m^n$ for several values of m provided a good indication of when n was sufficiently large; once uniformity of the $q_m^n$ values was obtained (for several m), further increases in n produced little change in the flux values.

The choice for initial values was $u_o(x,y) = \bar{y}-y$. Other choices of $U_o$ attempting to better approximate u(x,y) produced some instances of erratic and slow convergence of $U_{j,k}^n$ toward the steady state. The program was written so that a sequence of several different time steps could be run during the course of a single problem in order to obtain faster approach toward steady state values. With $D_f = 0$, k=2, tetragonal geometry, J=K=21, z=.02 and fiber volume fraction in the range 0 - .7, an appropriate sequence of time steps was found to be 40 steps with $\Delta t = .05$, followed by 20 steps with $\Delta t=20.0$, followed by 40 steps with $\Delta t=.5$. With $D_F=0$, k=2, hexagonal geometry, J=21, K=41, z=.02, and fiber volume fraction in the range 0-.85, an appropriate sequence of time steps was found to be 60 steps with $\Delta t=.02$, followed by 60 steps with $\Delta t=20.0$. Convergence tended to be more rapid with positive values of $D_f$ in (0,1). These choices of J,K, $\Delta t$, z were found by observing the effects of varying these parameters on the values of $d_e$ thus obtained.

## A5. A Numerical Example

We give results obtained from $D_f = 0$, k=2, hexagonal fiber geometry, J=21, K=41, z=.02, fiber volume fraction =.4, and the choices of $\Delta t$ stated above. Fluxes were calculated across $y_m = (m-1/2)\Delta y$ for m=1, 4, 10, 20, 40. The corresponding flux values at t=o (i.e. for $u_o$) were .3341, .3554, .4802, 1.0, .3341. After 60 steps with $\Delta t=.02$ the flux values were .4279, .4280, .4292, .4321, .4279. After 60 more steps with $\Delta t=20.0$ all five flux values were .4289.

## APPENDIX B

## Glossary

Symbols

| | |
|---|---|
| C,c | Indicating concentrations (at the boundary and at the interior respectively). |
| d | shortest distance from fiber to fiber surface |
| D,$\bar{d}$ | diffusion coefficient |
| $D_r$ | diffusion coefficient of the resin |
| $D_f$ | diffusion coefficient of the fiber |
| $\bar{D}$ | average diffusion coefficient |
| $D_e$, $d_e$ | effective diffusion coefficient |
| h | $\frac{1}{2}$ times the thickness of the composite plate |
| J | flux of diffusant |
| k | distribution coefficient |
| $k_m$ | thermal conductivity of the matrix |
| $k_f$ | thermal conductivity of the fiber |
| $K_m$ | electrical conductivity of the matrix |
| $\ell$ | thickness of the composite plate |
| q | flux (general) |
| $M_t$ | amount absorbed at time t |
| $M_\infty$ | amount absorbed after equilibrium has been reached |
| r | fiber radius |
| RH | relative humidity |

| | |
|---|---|
| t | time |
| ∥ | parallel |
| ⊥ | perpendicular |

Subscripts

Symbols Indicating

| | |
|---|---|
| e | effective |
| f | fiber |
| h | hexagonal |
| m | matrix |
| r | resin |
| t | tetragonal |
| ∥ | parallel |
| ⊥ | perpendicular |
| x | first derivative of the variable x |
| xx | second derivative of the variable x |
| y | first derivative of the variable y |
| yy | second derivative of the variable y |

DISTRIBUTION

Office of Director of Defense
Research and Engineering
Washington, D.C. 20301
Attn: Mr. J. Persh, OAD/ET — 1

Commander
Naval Air Systems Command
Washington, D.C. 20361
Attn: AIR 52032 (C. Bersch) — 1
AIR 53032D (M. Stander) — 1
AIR 320A (T. Kearns) — 1

Commander
Naval Sea Systems Command
Washington, D.C. 20360
Attn: SEA-033 — 1
SEA-035 — 1
SEA-09G32 — 2
SEA-03B — 1

Office of Naval Research
800 Quincy Street
Arlington, Virginia 22217
Code 472 (Dr. G. Neece) — 1
Code 470 (Dr. Edward I. Salkovitz) — 1

Office of Naval Research
495 Summer St.
Boston, MA 02210
Attn: Dr. L. Peebles — 1

Director
Naval Research Laboratory
Washington, D.C. 20375 — 2

Commander
Naval Weapons Center
China Lake, California 93555
Code 533 — 2

DISTRIBUTION

Commander
Naval Undersea Center
3202 E. Foothill Boulevard
Pasadena, California 91107

Director of Development
Army Material Command
Graveley Point
Washington, D.C. 20316 1

Commanding Officer
Picatinny Arsenal
Plastic Technical Evaluation Center
Dover, New Jersey 07801
Attn: A. M. Anzalone 1

Commanding Officer
U. S. Army Mobility Equipment
R & D Laboratory
Fort Belvoir, Virginia 22060
Attn: Technical Library 1

Air Force Materials Laboratory
Wright-Patterson Air Force Base
Ohio 45433
Attn: Techincal Library 1
S. W. Tsai 1
C. Browning 1
J. C. Halpin 1
D. Shirell 1

Commanding Officer
Army Materials and Mechanics
Research Center
Watertown, Massachusetts 02172
Attn: Library 1

Army Materials and Mechanics Research Center
Watertown, MA 02172
Attn: R. Sacher 1
J. Illinger 1
N. Schneider 1
G. Thomas 1
S. Wentworth 1

DISTRIBUTION

Commander
Naval Ship Research and Development Center
Carderock Library, Code 5641
Bethesda, Maryland 20032 — 1

Defense Documentation Center
Cameron Station
Alexandria, Virginia 22314 — 12

Commander
Naval Underwater Systems Center
Newport, Rhode Island 02840
Attn: LA151, Technical Library — 5

Director
Naval Avionics Facility
Indianapolis, Indiana 46218
Code 033 (C. Ferguson) — 1
Code 033.3 (W. W. Turner) — 1
Code 035 (Library) — 2

Commander
Naval Air Development Center
Warminister, Pennsylvania 18974
Attn: F. S. Williams — 1
W. Fegyna — 1
R. Trobacco — 1
Code 302 — 1

Director
Air Force Office of Scientific Research
1400 Wilson Boulevard
Arlington, Virginia 22209
Attn: SIGL — 1

Director
Strategic Systems Project Office
Washington, D.C. 20376
Attn: SP27312 (F. Vondersmith) — 1

DISTRIBUTION

| | |
|---|---|
| Federal Aviation Administration<br>Office of Super Sonic Development<br>800 Independence Avenue, S.W.<br>Washington, D.C. 20590 | |
| Attn: E. W. Bartholomew (SS-110) | 1 |
| NASA<br>Langley Research Center<br>Mail Stop 226<br>Langley Station<br>Hampton, Virginia 23365 | |
| Attn: Dr. Norman Johnston | 1 |
| Defense Nuclear Agency<br>Washington, D.C. 20305 | |
| Attn: Maj. R. Jackson | 1 |
| Mr. D. Kohler | 1 |
| Mr. J. Moulton | 1 |
| Air Force Weapons Laboratory<br>Kirtland Air Force Base<br>Alburquerque, New Mexico 87117 | 1 |
| Space and Missile Systems<br>Organization (AFSC)<br>Worldway Postal Center<br>P.O. Box 92960<br>Los Angeles, California 90009 | |
| Attn: Capt. J. Green | 1 |
| Capt. M. Elliot | 1 |
| Harry Diamond Laboratories<br>Washington, D.C. 20438 | |
| Attn: Library | 1 |
| Sandia Laboratories<br>Albuquerique, New Mexico 87115 | |
| Attn: Mr. D. Northrup | 1 |
| Aerospace Corporation<br>P.O. Box 92957<br>Los Angles, California 90009 | |
| Attn: Dr. R. A. Meyer | 1 |
| Dr. W. T. Barry | 1 |

DISTRIBUTION

AVCO Corporation
201 Lowell Street
Wilmington, Massachusetts 01887
Attn: Mr. C. K. Mullen 1
Mr. A. R. Taverna 1

Battelle Columbus Laboratories
505 King Avenue
Columbus, Ohio 43201
Attn: Mr. W. Pfeifer 1

Boeing Commercial Airplane Co.
P.O. Box 3707 M/S 73-43
Seattle, Washington 98124
Attn: J. T. Quinlivan 1

Effects Technology, Incorporated
5383 Hollister Avenue
Santa Barbara, California 93105
Attn: Mr. M. Graham 1
Mr. E. Steele 1

Kaman Sciences Corporation
P.O. Box 7463
Colorado Springs, Colorado 80933
Attn: Mr. J. C. Nickell 1

KTECH Corporation
P.O. Box 160
Goleta, California 93017
Attn: Mr. D. V. Keller 1

Lockheed Missiles and Space Company
P.O. Box 504
Sunnyvale, California 94088
Attn: Mr. A. Mietz 1

KTECH Corporation
911 Pennsylvania, Northeast
Albuquerque, New Mexico 87110
Attn: Larry Lee 1

DISTRIBUTION

Lockheed-Georgia Company
Dept. 72-26 Zone 28
Marietta, Georgia 30060
Attn: Walter S. Cremens 1

Los Alamos Scientific Laboratory
Los Alamos, New Mexico 87544
Attn: Dr. J. Taylor 1

Prototype Development Associates, Inc.
1740 Garry Avenue, Suite 201
Santa Ana, California 92705
Attn: Dr. John Slaughter 1

R & D Associates
P.O. Box 3580
Santa Monica, California 90403
Attn: Dr. R. A. Field 1

Southern Research Institute
2000 Ninth Avenue, South
Birmingham, Alabama 35205
Attn: Mr. C. D. Pears 1
Mr. James R. Brown 1

Systems, Science, and Software
P.O. Box 1620
La Jolla, California 92037
Attn: Dr. G. A. Gurtman 1

United Research Center
East Hartford, Connecticut 06601
Attn: D. A. Scola 1

Materials Science Corporation
Blue Bell, Pennsylvania 19422
Attn: B. W. Rosen 1

NDW-NSWC(W)-5605/1 (Rev. 1-75)

TO AID IN UPDATING THE DISTRIBUTION LIST FOR NAVAL SURFACE WEAPONS CENTER, WHITE OAK LABORATORY TECHNICAL REPORTS PLEASE COMPLETE THE FORM BELOW:

TO ALL HOLDERS OF NSWC/WOL/TR 76-7
by Joseph M. Augl, Code WR-31

DO NOT RETURN THIS FORM IF ALL INFORMATION IS CURRENT

A. FACILITY NAME AND ADDRESS *(OLD) (Show Zip Code)*

NEW ADDRESS *(Show Zip Code)*

B. ATTENTION LINE ADDRESSES:

C.

☐ REMOVE THIS FACILITY FROM THE DISTRIBUTION LIST FOR TECHNICAL REPORTS ON THIS SUBJECT.

D.
NUMBER OF COPIES DESIRED _____

GPO 886-870

DEPARTMENT OF THE NAVY
NAVAL SURFACE WEAPONS CENTER
WHITE OAK, SILVER SPRING, MD. 20910

OFFICIAL BUSINESS
PENALTY FOR PRIVATE USE, $300

POSTAGE AND FEES PAID
DEPARTMENT OF THE NAVY
DOD 316

COMMANDER
NAVAL SURFACE WEAPONS CENTER
WHITE OAK, SILVER SPRING, MARYLAND 20910

ATTENTION: CODE WR-31